Acta Crystallographica Section B
Structural Science
ISSN 0108-7681

Amino-substituted O^6-benzyl-5-nitrosopyrimidines: interplay of molecular, molecular-electronic and supramolecular structures

Antonio Quesada,[a,b] Antonio Marchal,[a] Manuel Melguizo,[a] Manuel Nogueras,[a] Adolfo Sánchez,[a] John N. Low,[b,c] Debbie Cannon,[b] Dorcas M. M. Farrell[d] and Christopher Glidewell[d]*

[a]Departamento de Química Inorgánica y Orgánica, Universidad de Jaén, 23071 Jaén, Spain, [b]School of Engineering, University of Dundee, Dundee DD1 4HN, Scotland, [c]Department of Chemistry, University of Aberdeen, Meston Walk, Old Aberdeen AB24 3UE, Scotland, and [d]School of Chemistry, University of St Andrews, St Andrews KY16 9ST, Scotland

Correspondence e-mail: cg@st-andrews.ac.uk

Received 26 November 2001
Accepted 17 December 2001

The structures of eight 2,4,6-trisubstituted-5-nitrosopyrimidines (one of which crystallizes in two polymorphs) have been determined, including seven O^6-benzyl derivatives which are potential, or proven, *in vitro* inhibitors of the human DNA-repair protein O^6-alkylguanine-DNA-transferase. In the derivatives having an amino substituent at the 4-position, an intramolecular N—H···O hydrogen bond with the nitroso O as an acceptor leads to an overall molecular shape similar to that of substituted purines. There is a marked propensity for these nitroso compounds to crystallize with $Z' = 2$. The structure of an analogue with no nitroso group is also reported for comparative purposes. Compounds containing the *N*-alkyl substituents —$NHCH_2COOEt$, —$NHCH_2CH_2COOEt$ and —$NHCH(CH_2Ph)COOEt$, derived from amino acid esters, exhibit a rich variety of conformational behaviour, and in all of the nitroso compounds the bond lengths provide strong evidence for a highly polarized electronic structure. Associated with this polarization is extensive charge-assisted hydrogen bonding between the molecules, leading to supramolecular aggregation in the form of finite (zero-dimensional) aggregates, chains, molecular ladders, sheets and frameworks.

1. Introduction

Of all the types of heteroaromatic compounds, the pyrimidines and their fused bicyclic analogues, the purines and pteridines are of particular interest on account of their diverse roles in biological systems. The important role that they play in biological processes, as nucleic acids constituents and enzyme cofactors, together with their use as therapeutic and diagnostic agents, make the preparation of new pyrimidine derivatives a permanent target for synthetic chemistry. 4-Amino-5-nitrosopyrimidines have long been important as intermediates for the synthesis of bicyclic azaheterocycles (Lister, 1996). More recently, their 6-alkoxy derivatives have been found to act as inhibitors of the human DNA-repair protein O^6-alkylguanine-DNA-transferase (AGT): thus, 2,4-diamino-6-benzyloxy-5-nitrosopyrimidine (1) has been shown (Chae *et al.*, 1995) to be a more potent *in vitro* inhibitor of AGT than the prototype inhibitor O^6-benzyloxyguanine (2), currently in clinical trials (Friedman *et al.*, 1998).

The use of newly developed synthetic methodology (Marchal *et al.*, 1998, 2000; Quesada *et al.*, 2000) gives ready access to a wide range of O^6-alkyl-5-nitrosopyrimidines as potential AGT inhibitors, and we present here a study of the molecular and supramolecular structures of seven such compounds (3)–(9), one of which crystallizes in two distinct monoclinic polymorphs (5*A*) and (5*B*), together with a study of an analogue (10) containing no nitroso substituent. By the use of *in vitro* assays performed on mutant *E. coli* strains

expressing human AGT (Abril *et al.*, 1999), (4) has already been shown to exhibit more potent AGT inhibition than the reference compound (2)

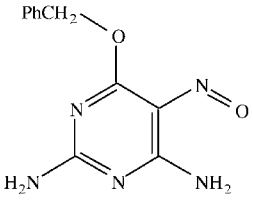

(1)

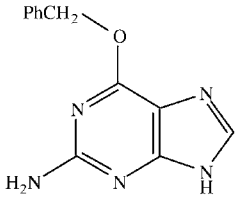

(2)

.

2. Experimental

2.1. Synthesis

2-Amino-4,6-dimethoxypyrimidine (purchased from Aldrich) was converted into (10) by reaction with sodium benzylate in benzyl alcohol, and (10) was subsequently converted into (3)–(9) and (11) using methods previously described (Marchal *et al.*, 1998, 2000; Quesada *et al.*, 2000). Crystals suitable for single-crystal X-ray diffraction were obtained from the following solvents: acetonitrile/ethanol/water (1/1/1 by volume), (3) as purple blocks, (5) as a mixture of blue plates [polymorph (5*A*)] and pink needles [polymorph (5*B*)], (6) as pink plates and (7) as pink plates; isopentanol (3-methyl-1-butanol) (4) as violet needles; dichloromethane/methanol (1/1 by volume), (8) as blue blocks; acetonitrile (9) as green blocks, (10) as colourless blocks and (11) as colourless plates: considerable difficulty was experienced in obtaining (11) in suitably crystalline form.

2.2. Data collection, structure solution and refinement

Diffraction data for (3)–(11) were collected at 150 (2) K using a Nonius Kappa-CCD diffractometer, using graphite-monochromated Mo $K\alpha$ radiation (λ = 0.71073 Å). Other details of cell data, data collection and refinement are summarized in Table 1, together with details of the software employed (Blessing, 1995, 1997; Ferguson, 1999; Nonius, 1997; Otwinowski & Minor, 1997; Sheldrick, 1997*a*,*b*; Spek, 2001).

For (3), (8) and (11) the space group $P2_1/n$ was uniquely assigned from the systematic absences; similarly, the space group $P2_1/c$ was uniquely assigned for (9). Two polymorphs were observed for (5) and both are monoclinic: for polymorph (5*A*), the space group $P2_1/c$ was uniquely assigned from the systematic absences; for polymorph (5*B*), the systematic absences permitted $P2_1$ and $P2_1/m$ as the possible space groups; $P2_1$ was chosen and subsequently confirmed by the successful structure analysis. For (10) the systematic absences permitted space groups Cc and $C2/c$; $C2/c$ was chosen and subsequently confirmed by the successful structure analysis. Compounds (4), (6) and (7) are all triclinic; for (4) and (7), the space group $P\bar{1}$ was selected and subsequently confirmed by the successful structure analysis, but space group $P1$ was chosen for (6) because the molecules are chiral. The structures were solved by direct methods and refined with all data on F^2. A weighting scheme based upon $P = [F_o^2 + 2F_c^2]/3$ was employed in order to reduce statistical bias (Wilson, 1976). All H atoms were located from difference maps and all were fully ordered: where H atoms of amino groups were found not to lie

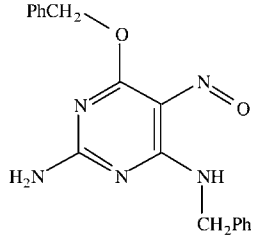

(3)

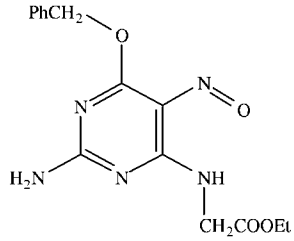

(4)

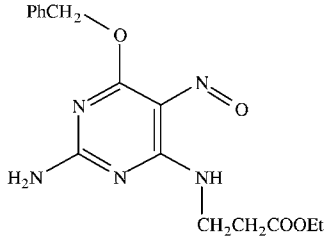

(5)

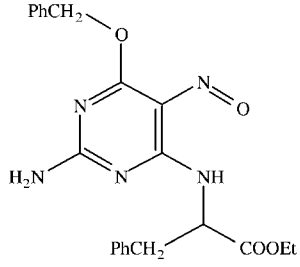

(6)

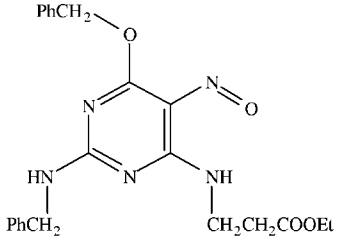

(7)

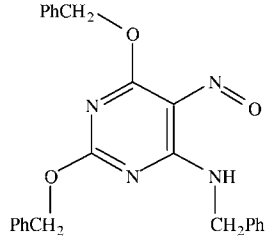

(8)

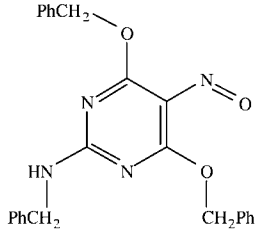

(9)

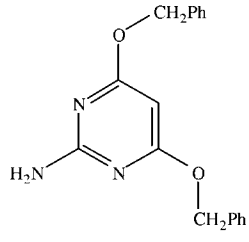

(10)

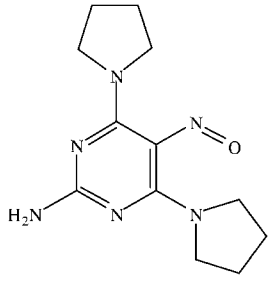

(11)

Table 1
Experimental details.

	(3)	(4)	(5*A*)	(5*B*)	(6)
Crystal data					
Chemical formula	$C_{18}H_{17}N_5O_2$	$C_{15}H_{17}N_5O_4$	$C_{16}H_{19}N_5O_4$	$C_{16}H_{19}N_5O_4$	$C_{22}H_{23}N_5O_4$
Chemical formula weight	335.37	331.34	345.36	345.36	421.45
Cell setting, space group	Monoclinic, $P2_1/n$	Triclinic, $P\overline{1}$	Monoclinic, $P2_1/c$	Monoclinic, $P2_1$	Triclinic, $P1$
a, b, c (Å)	11.677 (2), 13.362 (3), 21.478 (4)	7.3525 (4), 7.5420 (5), 14.9454 (13)	5.2399 (16), 31.1630 (14), 9.792 (4)	7.4830 (2), 16.6110 (6), 13.5378 (6)	7.9899 (3), 8.4278 (3), 17.0042 (7)
α, β, γ (°)	90, 102.58 (3), 90	91.797 (3), 100.467 (3), 106.102 (6)	90, 100.200 (12), 90	90, 91.5420 (11), 90	99.9100 (12), 90.5610 (13), 111.4880 (17)
V (Å^3)	3270.7 (11)	780.06 (10)	1573.7 (8)	1682.14 (11)	1046.22 (7)
Z	8	2	4	4	2
D_x (Mg m^{-3})	1.362	1.411	1.458	1.364	1.338
Radiation type	Mo $K\alpha$	Mo $K\alpha$	Mo $K\alpha$	Mo $K\alpha$	Mo $K\alpha$
No. of reflections for cell parameters	21 450	11 231	66 201	8888	14 344
θ range (°)	1.0–27.48	1.02–27.48	1.02–27.48	1.0–27.48	2.91–27.48
μ (mm^{-1})	0.093	0.105	0.108	0.101	0.095
Temperature (K)	150 (2)	150 (2)	150 (2)	150 (2)	150 (2)
Crystal form, colour	Block, purple	Needle, violet	Plate, blue	Needle, pink	Plate, pink
Crystal size (mm)	0.34 × 0.18 × 0.18	0.50 × 0.20 × 0.10	0.20 × 0.10 × 0.02	0.50 × 0.20 × 0.18	0.30 × 0.20 × 0.03
Data collection					
Diffractometer	Kappa-CCD	Kappa-CCD	Kappa-CCD	Kappa-CCD	Kappa-CCD
Data collection method	φ scans, and ω scans with κ offsets	φ scans, and ω scans with κ offsets	φ scans, and ω scans with κ offsets	φ scans, and ω scans with κ offsets	φ scans, and ω scans with κ offsets
Absorption correction	Multi-scan	Multi-scan	Multi-scan	Multi-scan	Multi-scan
T_{min}	0.9690	0.9492	0.9788	0.9513	0.9721
T_{max}	0.9834	0.9895	0.9978	0.9821	0.9972
No. of measured, independent and observed parameters	36 834, 7334, 4449	10 165, 3418, 1860	10 470, 2525, 822	19 365, 2992, 2487	14 846, 8664, 6321
Criterion for observed reflections	$I > 2\sigma(I)$	$I > 2\sigma(I)$	$I > 2\sigma(I)$	$I > 2\sigma(I)$	$I > 2\sigma(I)$
R_{int}	0.063	0.065	0.065	0.083	0.043
θ_{max} (°)	27.48	27.50	25.00	25.00	27.45
Range of h, k, l	$-14 \rightarrow h \rightarrow 14$ $-17 \rightarrow k \rightarrow 17$ $-27 \rightarrow l \rightarrow 27$	$-9 \rightarrow h \rightarrow 9$ $-9 \rightarrow k \rightarrow 9$ $-19 \rightarrow l \rightarrow 19$	$-6 \rightarrow h \rightarrow 6$ $-36 \rightarrow k \rightarrow 37$ $-11 \rightarrow l \rightarrow 11$	$-8 \rightarrow h \rightarrow 8$ $-19 \rightarrow k \rightarrow 19$ $-16 \rightarrow l \rightarrow 16$	$-10 \rightarrow h \rightarrow 10$ $-10 \rightarrow k \rightarrow 10$ $-22 \rightarrow l \rightarrow 22$
Refinement					
Refinement on	F^2	F^2	F^2	F^2	F^2
$R[F^2>2\sigma(F^2)]$, $wR(F^2)$, S	0.0515, 0.1495, 0.99	0.0551, 0.1638, 1.023	0.1059, 0.2829, 1.001	0.0551, 0.1492, 1.033	0.0455, 0.1095, 1.009
No. of reflections and parameters used in refinement	7334, 451	3418, 218	2525, 227	2992, 453	4686, 561
H-atom treatment	H-atom parameters constrained	H-atom parameters constrained	H-atom parameters constrained	H-atom parameters constrained	H-atom parameters constrained
Weighting scheme	$w = 1/[\sigma^2(F_o^2) + (0.0833P)^2]$, where $P = (F_o^2 + 2F_c^2)/3$	$w = 1/[\sigma^2(F_o^2) + (0.0778P)^2]$, where $P = (F_o^2 + 2F_c^2)/3$	$w = 1/[\sigma^2(F_o^2) + (0.0757P)^2 + 2.3684P]$, where $P = (F_o^2 + 2F_c^2)/3$	$w = 1/[\sigma^2(F_o^2) + (0.1159P)^2]$, where $P = (F_o^2 + 2F_c^2)/3$	$w = 1/[\sigma^2(F_o^2) + (0.0638P)^2]$, where $P = (F_o^2 + 2F_c^2)/3$
$(\Delta/\sigma)_{max}$	0.001	0.000	0.002	0.004	0.001
$\Delta\rho_{max}, \Delta\rho_{min}$ (e Å^{-3})	0.301, −0.406	0.385, −0.512	0.231, −0.219	0.555, −0.331	0.195, −0.246

	(7)	(8)	(9)	(10)	(11)
Crystal data					
Chemical formula	$C_{23}H_{25}N_5O_4$	$C_{25}H_{22}N_4O_3$	$C_{25}H_{22}N_4O_3$	$C_{18}H_{17}N_3O_2$	$C_{24}H_{38.20}N_{12}O_{3.10}$
Chemical formula weight	435.48	426.47	426.47	307.35	544.47
Cell setting, space group	Triclinic, $P\overline{1}$	Monoclinic, $P2_1/n$	Monoclinic, $P2_1/c$	Monoclinic, C_2/c	Monoclinic, $P2_1/n$
a, b, c (Å)	8.6595 (2), 16.3567 (4), 16.9014 (4)	14.6856 (5), 7.7726 (2), 18.5721 (8)	13.8074 (3), 15.8175 (5), 10.2119 (5)	32.4902 (9), 7.5034 (2), 12.7804 (4)	18.4687 (8), 8.1067 (3), 19.1880 (6)

Table 1 (continued)

	(7)	(8)	(9)	(10)	(11)
α, β, γ (°)	105.2210 (13), 104.6960 (13), 100.3720 (12)	90, 99.8847 (13), 90	90, 105.7490 (11), 90	90, 98.8790 (16), 90	90, 110.580 (2), 90
V (Å^3)	2154.95 (9)	2088.45 (13)	2146.54 (13)	3078.36 (15)	2689.50 (17)
Z	4	4	4	8	4
D_x (Mg m^{-3})	1.342	1.356	1.320	1.326	1.345
Radiation type	Mo $K\alpha$	Mo $K\alpha$	Mo $K\alpha$	Mo $K\alpha$	Mo $K\alpha$
No. of reflections for cell parameters	9402	3748	10 763	3482	4758
θ range (°)	1.32–27.48	1.0–27.47	1.0–27.48	2.54–27.47	1.31–24.99
μ (mm^{-1})	0.094	0.091	0.089	0.089	0.095
Temperature (K)	150 (2)	150 (2)	150 (2)	150 (2)	150 (2)
Crystal form, colour	Plate, pink	Block, blue	Prism, green	Block, colourless	Plate, colourless
Crystal size (mm)	0.40 × 0.40 × 0.05	0.55 × 0.30 × 0.20	0.30 × 0.24 × 0.12	0.40 × 0.40 × 0.26	0.20 × 0.20 × 0.07
Data collection					
Diffractometer	Kappa-CCD	Kappa-CCD	Kappa-CCD	Kappa-CCD	Kappa-CCD
Data collection method	φ scans, and ω scans with κ offsets	φ scans, and ω scans with κ offsets	φ scans, and ω scans with κ offsets	φ scans, and ω scans with κ offsets	φ scans and ω scans with κ offsets
Absorption correction	Multi-scan	Multi-scan	Multi-scan	Multi-scan	Multi-scan
T_{min}	0.9632	0.9515	0.9738	0.9654	0.9813
T_{max}	0.9953	0.9820	0.9894	0.9773	0.9934
No. of measured, independent and observed parameters	33 749, 9402, 5874	12 659, 4516, 3296	18 529, 4857, 3078	13 174, 3482, 2677	50 212, 4758, 3200
Criterion for observed reflections	$I > 2\sigma(I)$	$I > 2\sigma(I)$	$I > 2\sigma(I)$	$I > 2\sigma(I)$	$I > 2\sigma(I)$
R_{int}	0.092	0.046	0.075	0.044	0.060
θ_{max} (°)	27.48	27.47	27.48	27.47	25.00
Range of h, k, l	$-11 \rightarrow h \rightarrow 11$ $-21 \rightarrow k \rightarrow 21$ $-20 \rightarrow l \rightarrow 21$	$-19 \rightarrow h \rightarrow 19$ $-10 \rightarrow k \rightarrow 10$ $-23 \rightarrow l \rightarrow 24$	$-17 \rightarrow h \rightarrow 17$ $-20 \rightarrow k \rightarrow 17$ $-13 \rightarrow l \rightarrow 13$	$-40 \rightarrow h \rightarrow 42$ $-8 \rightarrow k \rightarrow 9$ $-16 \rightarrow l \rightarrow 15$	$-21 \rightarrow h \rightarrow 21$ $-8 \rightarrow k \rightarrow 9$ $-22 \rightarrow l \rightarrow 22$
Refinement					
Refinement on	F^2	F^2	F^2	F^2	F^2
$R[F^2>2\sigma(F^2)]$, $wR(F^2)$, S	0.0667, 0.186, 0.99	0.0473, 0.1314, 1.065	0.0508, 0.1263, 1.011	0.0442, 0.115, 1.044	0.0761, 0.2362, 1.008
No. of reflections and parameters used in refinement	9402, 579	4516, 289	4857, 289	3482, 208	4758, 391
H-atom treatment	H-atom parameters constrained	H-atom parameters constrained	H-atom parameters constrained	H-atom parameters constrained	H-atom parameters constrained
Weighting scheme	$w = 1/[\sigma^2(F_o^2) + (0.1133P)^2]$, where $P = (F_o^2 + 2F_c^2)/3$	$w = 1/[\sigma^2(F_o^2) + (0.0762P)^2]$ where $P = (F_o^2 + 2F_c^2)/3$	$w = 1/[\sigma^2(F_o^2) + (0.0662P)^2]$, where $P = (F_o^2 + 2F_c^2)/3$	$w = 1/[\sigma^2(F_o^2) + (0.0613P)^2 + 0.8375P]$, where $P = (F_o^2 + 2F_c^2)/3$	$w = 1/[\sigma^2(F_o^2) + (0.1429P)^2 + 1.8403P]$, where $P = (F_o^2 + 2F_c^2)/3$
$(\Delta/\sigma)_{max}$	0.000	0.000	0.000	0.001	0.000
$\Delta\rho_{max}, \Delta\rho_{min}$ (e Å^{-3})	0.431, −0.507	0.261, −0.329	0.218, −0.335	0.198, −0.268	0.524, −0.348

in the plane of the adjacent heteroaromatic ring, they were treated using *DFIX* commands in *SHELXL*97, followed by AFIX; otherwise they were included in the refinements as riding atoms with N—H 0.86–0.94, C—H 0.95 (aromatic), 0.98 (CH_3), 0.99 (CH_2) or 1.00 Å (aliphatic C—H). For (5*B*) and (6) the refined values [−0.9 (10) and 1.6 (16), respectively] of the Flack parameter (Flack, 1983) were inconclusive (Flack & Bernardinelli, 2000) and hence for both compounds the Friedel equivalents were merged before the final refinements. The overall precision of the structure determination for the blue $P2_1/c$ polymorph (5*B*) of (5) is rather low: even at 150 (2) K the proportion of the reflections labelled 'observed' is less than 33% and the fall-off of intensity with θ is such that data collection was terminated at $\theta = 25°$. For (6) the chirality was set by reference to the known (*S*) configuration at atoms C17 and C27. In (11) the coordinates of the two independent molecules were related by an approximate A-centring relationship, although a careful search for possible additional symmetry showed that $P2_1/n$ was indeed the correct space group: in particular, *hkl* reflections having $(k + l)$ odd were present, although generally weak. In both molecules the nitroso group is disordered over two sets of sites; for each molecule the site-occupation factors (s.o.f.s) for the two sets of sites were constrained to sum to unity, but the s.o.f.s for the two molecules were allowed to refine independently. In addition to the evident disorder of the nitroso groups, there were indications of orientational disorder in several of the puckered pyrrolidine rings, although it was possible to model

this satisfactorily only for one of the rings. As well as two molecules of (11), the structure also contained two partially occupied water sites containing O1 and O2, respectively, whose refined s.o.f.s are 0.902 (9) and 0.196 (9), respectively. In one of the pyrrolidine rings one C atom was modelled with two sites, denoted C143 and C14*B* and with the s.o.f.s constrained to sum to unity; these refined to 0.796 (7) and 0.204 (7), respectively; since the C14*B* and O2 sites cannot both be occupied in the same asymmetric unit as their contact distance would be only *ca* 2.60 Å, it seems likely that there is correlated disorder here: O2 is present when site C143 is occupied and absent when site C14*B* is occupied. Because of this, and the effectively identical values of the refined s.o.f.s for C14*B* and O2, these values were fixed at 0.20 in the final refinements, with that of C143 fixed accordingly at 0.80. The combination of the pseudosymmetry and the multiple disorder, together with the consistently poor quality of the diffraction data (R_{int} = 0.102, probably connected with the difficulty experienced in obtaining crystalline material), indicate that the refinement of (11) is at the margin of tractability. In an attempt to circumvent these problems by the use of similar compounds in which the secondary amino components are not subject to such disorder, the corresponding bis-(1-piperidino), bis-(4-morpholino) and bis-(dimethylamino)

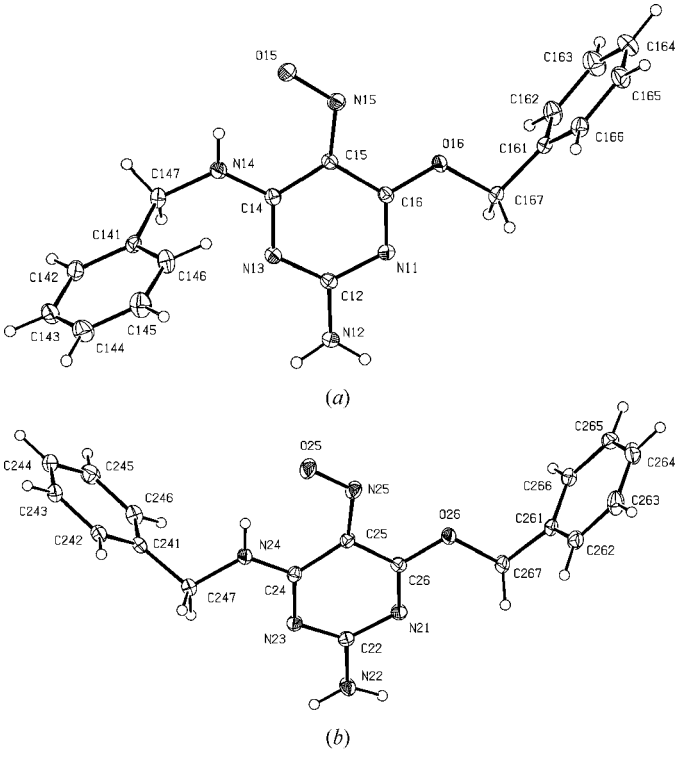

Figure 1
The two independent molecules in (3), showing the atom-labelling scheme. Displacement ellipsoids are drawn at the 30% probability level.

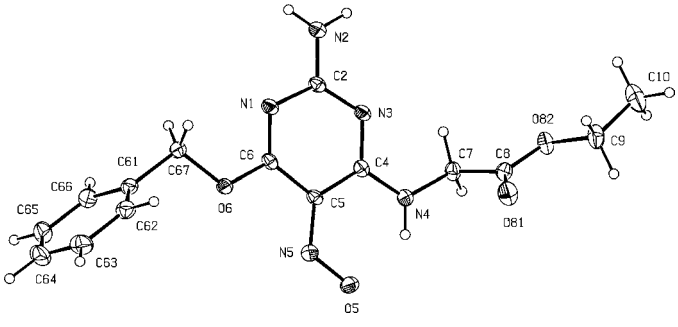

Figure 2
A molecule of (4), showing the atom-labelling scheme. Displacement ellipsoids are drawn at the 30% probability level.

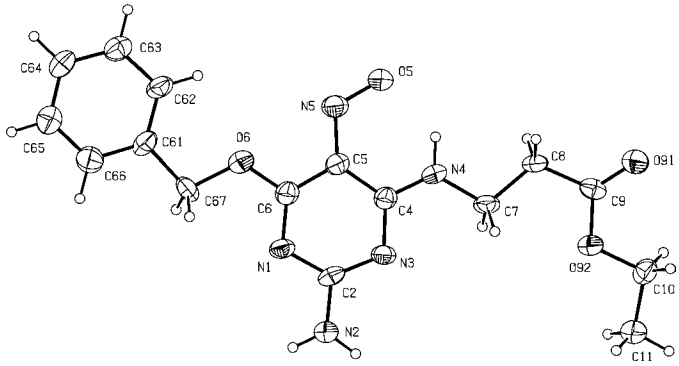

Figure 3
A molecule of (5) in the $P2_1/c$ polymorph (5*A*), showing the atom-labelling scheme. Displacement ellipsoids are drawn at the 30% probability level.

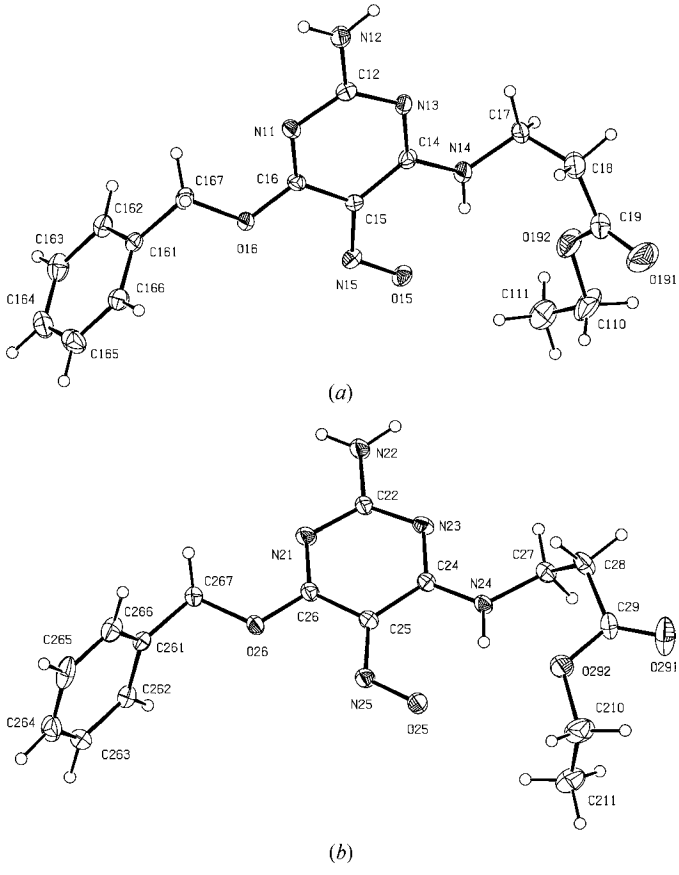

Figure 4
The two independent molecules of (5) in the $P2_1$ polymorph (5*B*), showing the atom-labelling scheme. Displacement ellipsoids are drawn at the 30% probability level.

Table 2
Torsional angles (°) in nitroso compounds involving benzyl substituents.

	(3)		(4)	(5*A*)	(5*B*)	
	n = 1	*n* = 2	*n* = nil	*n* = nil	*n* = 1	*n* = 2
N*n*1—C*n*2—N*n*2—C*n*27	–	–	–	–	–	–
C*n*5—C*n*4—N*n*4—C*n*47	171.2 (2)	−178.2 (2)	179.5 (2)†	177.9 (8)†	−179.2 (4)†	179.4 (4)†
C*n*4—C*n*5—N*n*5—O*n*5	2.4 (3)	0.3 (3)	−2.1 (3)	−1.8 (14)	−1.0 (6)	1.8 (6)
C*n*5—C*n*6—O*n*6—C*n*67	−174.6 (2)	173.5 (2)	−176.8 (2)	179.4 (9)	−174.4 (3)	177.5 (4)
C*n*2—N*n*2—C*n*27—C*n*41	–	–	–	–	–	–
C*n*4—N*n*4—C*n*47—C*n*41	83.8 (2)	−139.8 (2)	108.2 (2)‡	−175.7 (9)‡	112.8 (5)‡	126.5 (4)‡
C*n*6—O*n*6—C*n*67—C*n*61	165.7 (2)	−172.4 (2)	170.6 (2)	179.0 (8)	166.7 (3)	−176.2 (4)

	(6)		(7)		(8)	(9)
	n = 1	*n* = 2	*n* = 1	*n* = 2	*n* = nil	*n* = nil
N*n*1—C*n*2—N*n*2—C*n*27	–	–	−173.2 (2)	176.7 (2)	178.6 (2)§	−178.4 (2)
C*n*5—C*n*4—N*n*4—C*n*47	173.3 (2)†	−170.3 (3)†	−175.3 (2)†	−176.7 (2)†	179.4 (2)	178.6 (2)¶
C*n*4—C*n*5—N*n*5—O*n*5	1.2 (4)	−1.5 (5)	−1.5 (3)	−0.9 (3)	−1.3 (2)	1.7 (2)
C*n*5—C*n*6—O*n*6—C*n*67	176.5 (2)	−179.0 (3)	179.6 (2)	173.8 (2)	176.9 (2)	−178.2 (2)
C*n*2—N*n*2—C*n*27—C*n*41	–	–	−76.1 (3)	76.6 (3)	−167.2 (2)††	75.4 (2)
C*n*4—N*n*4—C*n*47—C*n*41	−70.8 (4)‡	−76.9 (4)‡	80.2 (3)‡	92.3 (2)‡	95.1 (2)	−179.6 (2)‡‡
C*n*6—O*n*6—C*n*67—C*n*61	−84.4 (3)	116.3 (3)	172.6 (2)	−164.1 (2)	168.2 (2)	−81.6 (2)

† C*n*5—C*n*4—N*n*4—Cn7. ‡ C*n*4—N*n*4—C*n*7—C*n*8. § N1—C2—O1—C27. ¶ C5—C4—O4—C47. †† C2—O1—C27—C21. ‡‡ C4—O4—C47—C41.

Table 3
Torsional angles (°) involving aliphatic side chains in (5*A*), (5*B*) and (7).

	(5*A*)	(5*B*)		(7)	
	n = nil	*n* = 1	*n* = 2	*n* = 1	*n* = 2
C*n*4—N*n*4—C*n*7—C*n*8	−175.7 (9)	112.8 (5)	126.5 (5)	80.2 (3)	92.3 (2)
N*n*4—C*n*7—C*n*8—C*n*9	175.0 (8)	63.1 (5)	69.2 (5)	168.1 (2)	69.8 (2)
C*n*7—C*n*8—C*n*9—O*n*91	−172.2 (9)	−179.3 (6)	123.9 (5)	2.1 (3)	1.7 (3)
C*n*7—C*n*8—C*n*9—O*n*92	9.4 (12)	−0.6 (6)	−61.7 (5)	−177.6 (2)	−179.1 (3)
C*n*8—C*n*9—O*n*92—C*n*10	175.3 (7)	−175.9 (5)	177.6 (5)	179.5 (2)	−179.5 (2)
C*n*9—O*n*92—C*n*10—C*n*11	−175.1 (8)	173.8 (5)	−103.5 (5)	174.4 (2)	−174.7 (2)

analogues of (11) have all been examined, but none of these has been obtained in suitably crystalline form.

Supramolecular analyses were made with the aid of *PLATON* (Spek, 2001) and the diagrams were prepared with the aid of *PLATON* (Spek, 2001). Figs. 1–10 show the molecular structures of (3)–(11), with the atom-labelling schemes, and Figs. 11–25 show aspects of the supramolecular structures. Selected molecular dimensions are presented in Tables 2–6 and details of the hydrogen bonding are given in Table 7.[1]

3. Results and discussion

3.1. Crystallization characteristics

Compounds (3)–(7) are all characterized by amino substituents at positions 2 and 4, with a benzyloxy substituent at position 6. Compounds (8) and (9) differ from the series (3)–(7) in that (8) and (9) both carry benzyloxy substituents at positions 2 and 4, respectively, in addition to that at position 6. It is striking that (3), (5)–(7) and (11) all crystallize in forms having $Z' = 2$: in every case the conformations of the two independent molecules differ significantly (see §3.2 below) and this alone is sufficient to preclude any additional symmetry. Moreover, (5) crystallizes in two polymorphic forms, both monoclinic: (5*A*) in space group $P2_1/c$ with $Z' = 1$ and (5*B*) in space group $P2_1$ with $Z' = 2$, and none of the three independent conformers of (5) resembles the other two (Figs. 3 and 4).

3.2. Molecular conformations

In each of (3)–(9) the nitroso group is essentially coplanar with the pyrimidine ring and in (3)–(8) there is an intramolecular N—H···O hydrogen bond having the nitroso O as an acceptor, which doubtless reinforces this tendency to coplanarity. There is thus a clear similarity in overall molecular shape between 4-amino-5-nitrosopyrimidines (I) on the one hand and purines (II) on the other.

In the 6-benzyloxy substituents the CH_2 carbon is also nearly coplanar with the pyrimidine ring, with the torsional angle C*n*5—C*n*6—O*n*6—C*n*67 (Figs. 1–9) always within ±7° of 180°, and oriented

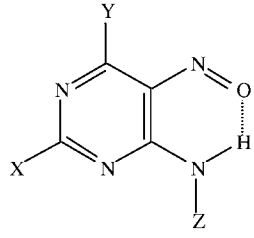

(I)

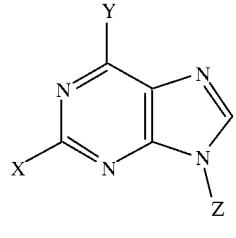

(II)

such that the 6-benzyloxy and the 5-nitroso groups are directed away from one another (Table 2). On the other hand, the *ipso* C of the associated aromatic ring is sometimes far removed from this plane, as indicated by the values of the torsional angles C*n*6—O*n*6—C*n*67—C*n*61 in (6), for example: however, in (3)–(5), (7) and (8) these torsional angles do not deviate from 180° by more than 20°. In (10), where there is no nitroso group, the molecule is almost planar: the C5—C*n*—O*n*—C*n*7 torsional angles are 177.4 (2) and 2.0 (2)° for *n* = 4 or 6, respectively, and the corresponding C*n*—O*n*—C*n*7—C*n*1 angles are −176.0 (2) and 179.2 (2)°, respectively.

The most notable aspects of the molecular conformations in this series are manifested in the behaviour of the aliphatic side chains in (4)–(7). Compounds (5) and (7) both contain a

[1] Supplementary data for this paper are available from the IUCr electronic archives (Reference: NA0133). Services for accessing these data are described at the back of the journal.

$-CH_2CH_2COOEt$ substituent at N4: (5) crystallizes in two polymorphs and polymorph (5*B*) has $Z' = 2$, and likewise (7) crystallizes with $Z' = 2$, so that (5) and (7) between them provide five independent molecules containing the $-CH_2CH_2COOEt$ substituent. In the atom sequence from C*n*4 to C*n*11 (Table 3), there are five independent torsional angles and from these it is clear that no two molecules have the same conformation for this substituent. This is most readily summarized by classifying the torsional angles as antiperiplanar (*ap*) and so on: these torsional characteristics confirm that all five examples have completely different conformations. Similarly, in (4) and (6) (which has $Z' = 2$), the three examples of $-CHRCOOEt$ side chains [where R = H in (4) and $PhCH_2$ in (6)] all have different conformations (Table 4). It may be concluded that this rich conformational variety is a consequence of the essentially complete flexibility of these substituents, with very small energy barriers to rotation about the single N—C, C—C and C—O bonds, and that the precise folding of the side chains is probably constrained largely by the intermolecular interactions, particularly the hard hydrogen bonds which dominate the molecular packing and the supramolecular aggregation.

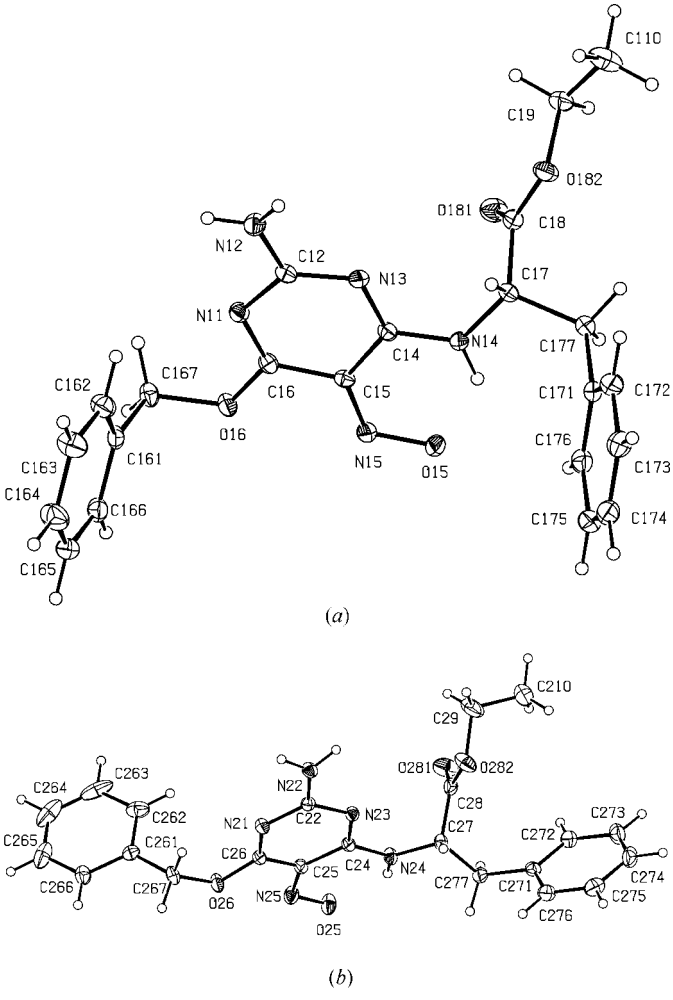

Figure 5
The two independent molecules in (6), showing the atom-labelling scheme. Displacement ellipsoids are drawn at the 30% probability level.

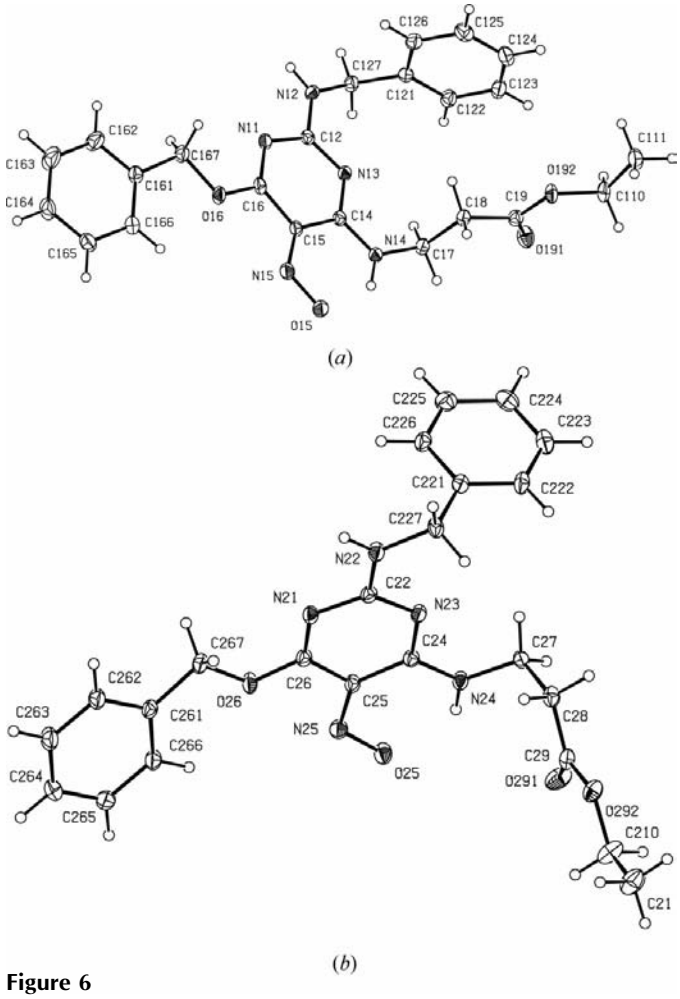

Figure 6
The two independent molecules in (7), showing the atom-labelling scheme. Displacement ellipsoids are drawn at the 30% probability level.

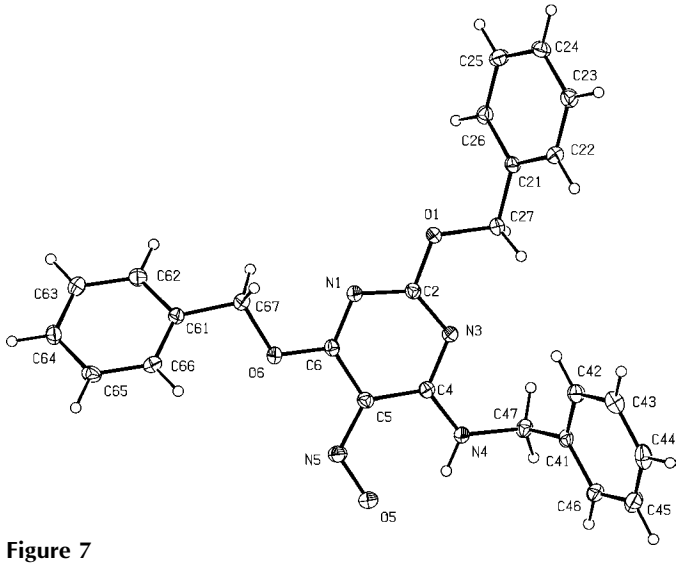

Figure 7
A molecule of (8), showing the atom-labelling scheme. Displacement ellipsoids are drawn at the 30% probability level.

Table 4
Torsional angles (°) involving aliphatic side chains in (4) and (6).

	(4)	(6)	
	n = nil	n = 1	n = 2
Cn4—Nn4—Cn7—Cn8	108.0 (2)	−70.8 (4)	−76.9 (4)
Nn4—Cn7—Cn8—On81	3.9 (4)	−17.0 (4)	−52.2 (4)
Nn4—Cn7—Cn8—On82	−175.9 (2)	166.9 (2)	127.6 (3)
Cn7—Cn8—On82—Cn9	175.4 (2)	173.8 (2)	−175.3 (3)
Cn8—On82—Cn9—Cn10	−172.9 (2)	−173.0 (3)	−87.6 (5)
Cn4—Nn4—Cn7—Cn77	–	170.2 (3)	162.4 (3)
Nn4—Cn7—Cn77—Cn71	–	−68.9 (3)	−171.6 (3)

In both the independent molecules in (11) the pyrimidine rings are seriously puckered, and the nitroso O atoms (in both orientations of the disordered nitroso substituent) are not coplanar with the adjacent C—C—N fragments (Table 5). This may reasonably be ascribed to the influence of the pyrollidine ring substituents at positions 4 and 6. There is now no possibility of an intramolecular N—H···O hydrogen bond to the O of the nitroso group; in addition, there is serious competition between electronic and steric factors. Maximum π-overlap between, on the one hand, the ring orbitals and, on the other, the orbitals of the nitroso group and of the planar N of the pyrrolidine substituents requires all of these orbitals to be parallel, which in turn requires both planarity of the pyrimidine ring and coplanarity with this ring of the C—N═O and C—NR_2 substituent groups. This requirement would, however, lead to a number of unreasonably short nonbonded contacts between atoms in the various substituents, in particular between nitroso group and the CH_2 groups of the pyrrolidines. There is some indication that some of the C atoms in the pyrollidine rings may also be mobile and/or disordered, but no satisfactory model for this could be developed: in view of the extensive disorder in this compound, the bond lengths and the electronic structure will not be discussed further in §3.3 below.

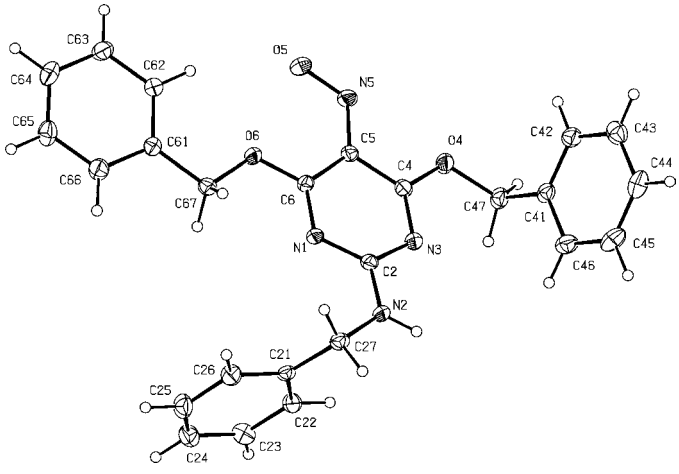

Figure 8
A molecule of (9), showing the atom-labelling scheme. Displacement ellipsoids are drawn at the 30% probability level.

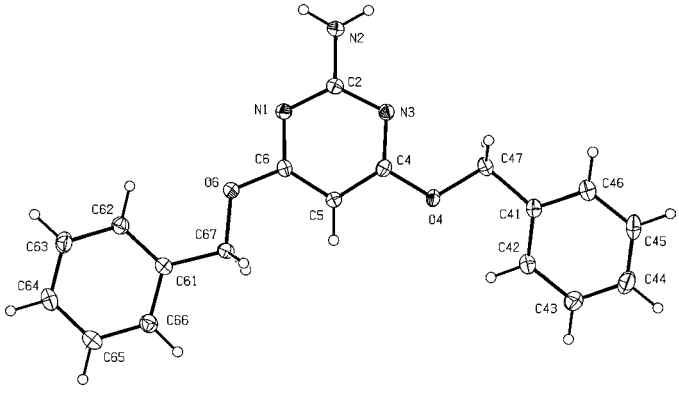

Figure 9
A molecule of (10), showing the atom-labelling scheme. Displacement ellipsoids are drawn at the 30% probability level.

3.3. Intermolecular bond lengths

The bond distances in the heteroaromatic rings and their immediate substituents display a number of patterns. We consider first those examples, (3)–(7), with amino substituents

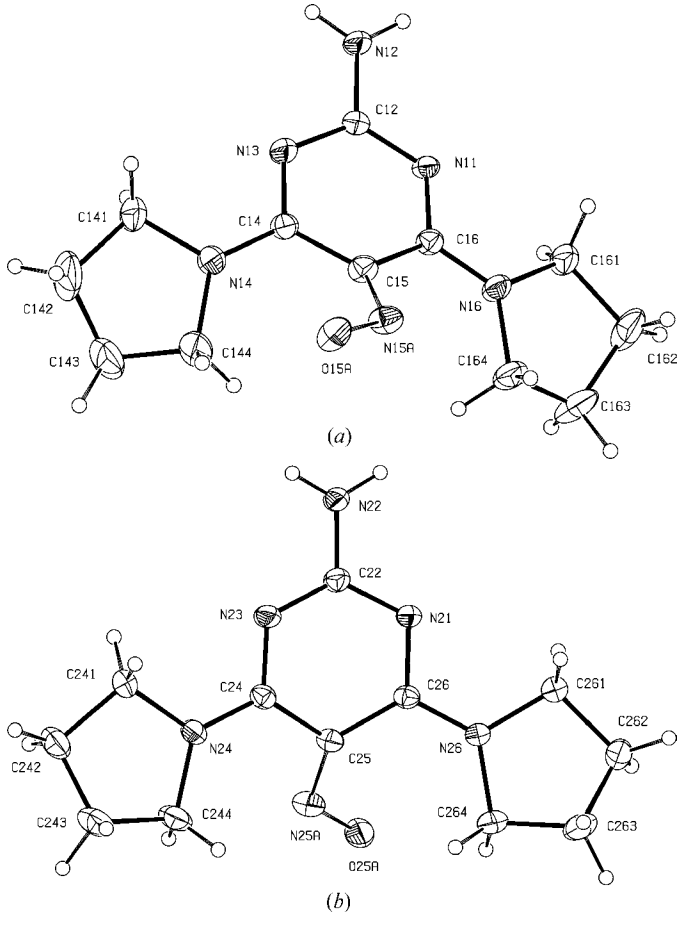

Figure 10
The two independent molecules in (11), showing the atom-labelling scheme. Displacement ellipsoids are drawn at the 30% probability level. For the sake of clarity, only the major components are shown.

Table 5
Selected torsional angles (°) in (11).

	n = 1	*n* = 2
N*n*1—C*n*2—N*n*3—C*n*4	11.7 (6)	14.0 (5)
C*n*2—N*n*3—C*n*4—C*n*5	10.9 (5)	1.9 (4)
N*n*3—C*n*4—C*n*5—C*n*6	−25.8 (4)	−17.8 (4)
C*n*4—C*n*5—C*n*6—N*n*1	20.8 (4)	20.9 (4)
C*n*5—C*n*6—N*n*1—C*n*2	−1.7 (4)	−7.7 (4)
C*n*6—N*n*1—C*n*2—N*n*3	−16.3 (5)	−11.0 (5)
N*n*3—C*n*4—C*n*5—N*n*5*A*	143.7 (4)	147.0 (3)
C*n*4—C*n*5—N*n*5*A*—O*n*5*A*	−2.0 (6)	−162.8 (3)
C*n*6—C*n*5—N*n*5*A*—O*n*5*A*	167.4 (3)	−0.6 (5)

Table 6
Selected intramolecular distances for (3)–(10) (Å).

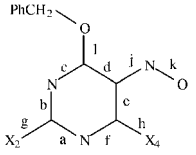

	a	*b*	*c*	*d*	*e*	*f*
(3)	1.337 (2)	1.369 (2)	1.306 (2)	1.436 (3)	1.445 (2)	1.339 (2)
	1.344 (2)	1.366 (2)	1.298 (2)	1.426 (2)	1.454 (2)	1.338 (2)
(4)	1.339 (3)	1.368 (3)	1.306 (3)	1.428 (3)	1.436 (3)	1.332 (3)
(5*A*)	1.351 (11)	1.368 (10)	1.317 (10)	1.386 (12)	1.427 (11)	1.345 (9)
(5*B*)	1.342 (5)	1.383 (5)	1.304 (5)	1.435 (6)	1.441 (5)	1.336 (5)
	1.333 (5)	1.371 (5)	1.301 (5)	1.427 (5)	1.450 (5)	1.340 (5)
(6)	1.344 (4)	1.371 (4)	1.303 (4)	1.433 (4)	1.442 (4)	1.331 (4)
	1.356 (4)	1.359 (4)	1.303 (4)	1.441 (4)	1.441 (4)	1.324 (4)
(7)	1.345 (3)	1.376 (3)	1.298 (3)	1.440 (3)	1.448 (3)	1.330 (3)
	1.341 (3)	1.378 (3)	1.299 (3)	1.435 (3)	1.446 (3)	1.332 (3)
(8)	1.317 (2)	1.347 (2)	1.315 (2)	1.425 (2)	1.439 (2)	1.352 (2)
(9)	1.349 (2)	1.358 (2)	1.319 (2)	1.425 (2)	1.423 (2)	1.311 (2)
(10)	1.355 (2)	1.337 (2)	1.335 (3)	1.378 (2)	1.393 (2)	1.313 (2)

	g	*h*	*j*	*k*	*l*	Δ
(3)	1.322 (2)	1.326 (2)	1.344 (2)	1.277 (2)	1.339 (2)	0.067 (2)
	1.319 (2)	1.324 (2)	1.347 (2)	1.275 (2)	1.335 (2)	0.072 (2)
(4)	1.312 (3)	1.329 (3)	1.352 (3)	1.275 (2)	1.337 (3)	0.077 (3)
(5*A*)	1.325 (9)	1.310 (10)	1.369 (9)	1.264 (9)	1.346 (9)	0.105 (9)
(5*B*)	1.314 (5)	1.330 (6)	1.346 (5)	1.277 (4)	1.338 (4)	0.069 (5)
	1.327 (5)	1.320 (5)	1.345 (5)	1.276 (4)	1.340 (4)	0.069 (5)
(6)	1.327 (4)	1.334 (4)	1.336 (4)	1.289 (3)	1.335 (4)	0.047 (4)
	1.318 (4)	1.334 (4)	1.332 (4)	1.292 (3)	1.327 (4)	0.040 (4)
(7)	1.325 (3)	1.335 (3)	1.340 (3)	1.294 (3)	1.336 (3)	0.046 (3)
	1.324 (3)	1.335 (3)	1.345 (3)	1.288 (3)	1.339 (3)	0.057 (3)
(8)	1.334 (2)	1.324 (2)	1.358 (2)	1.272 (2)	1.332 (2)	0.086 (2)
(9)	1.328 (2)	1.320 (2)	1.367 (2)	1.251 (2)	1.331 (2)	0.116 (2)
(10)	1.346 (2)	1.356 (2)	–	–	1.352 (2)	–

Substituents *X*2 and *X*4 are as defined in Scheme 2; bond *g* in (8) and bond *h* in (9) and (10) are C—O rather than C—N; the NO substituent is absent in (10).

at both the 2- and 4-positions, and then those with a second benzyloxy substituent at either the 2- or the 4-position.

Firstly, in (3)–(7) the sequence of C—N bonds labelled *a*, *f*, *g* and *h* in Table 6 show very little variation in length between those which are formally single (exterior to the rings) and those which might be either double or aromatic delocalized (those within the rings). Secondly, bonds *b* and *f* are of similar length, while bond *c* is always much shorter than bond *b*. Finally, bonds *j* and *k* are similar in length, although in simple neutral compounds where there is no possibility of significant electronic delocalization these distances normally differ by at least 0.20 Å (Talberg, 1977; Schlemper *et al.*, 1986) and the NO distance rarely exceeds 1.25 Å (Davis *et al.*, 1965; Bauer & Andreassen, 1972; Talberg, 1977; Schlemper *et al.*, 1986). These observations taken together confirm the polarized form (*B*) as the dominant contributor to the overall electronic structure, rather than the classical charge-localized form (*A*):

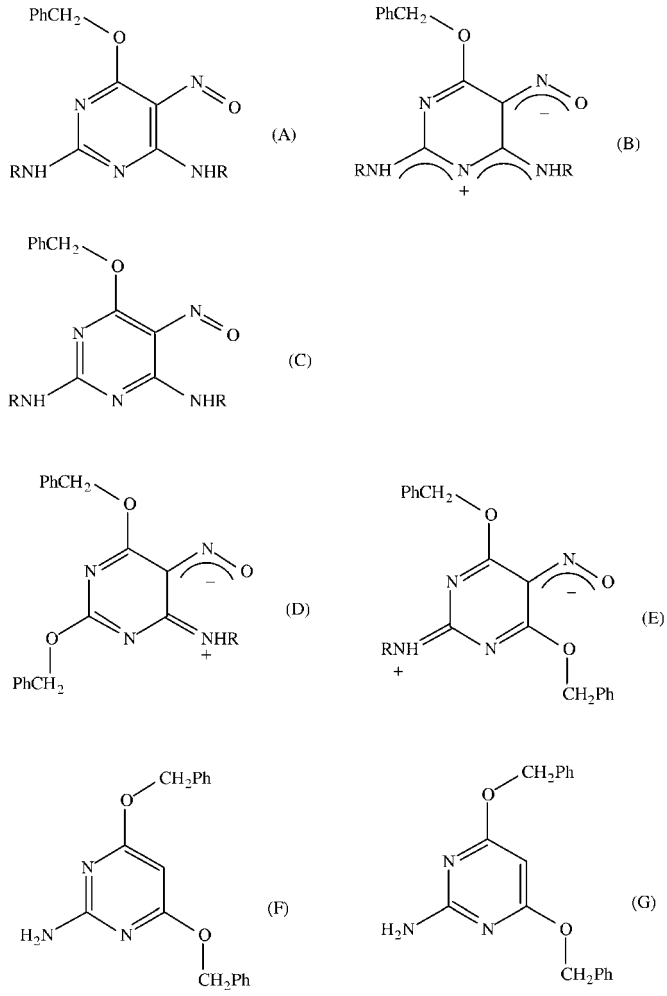

at the same time, the alternative formulation (*C*) can be ruled out by consideration of the relative magnitudes of the bond lengths for *c* and *d*.

By contrast, in (8), where the 2-substituent is a benzyloxy group rather than an amino group, bond *f* is significantly longer than in (3)–(7), while bond *h* is somewhat shorter: the previously observed patterns for bonds *b* and *c*, and for *j* and *k*, persist. On the other hand, in (9) where the additional benzyloxy substituent is at the 4-position, bond *a* is much longer than usual, while bond *f* is short: the *b*/*c* and *j*/*k* bond pairs show the usual behaviour. Overall these patterns of bond distances point to the polar forms (*D*) and (*E*) as the dominant contributors to the electronic structures of (8) and (9), respectively.

In (10) there is no nitroso group and hence no possibility of charge-separated polar forms analogous to (*A*), (*D*) and (*E*): to that extent (10) acts as a reference point against which to judge the validity of the deductions made above concerning (3)–(9). The conformation adopted by the benzyloxy groups in (10) precludes the obvious possibility of twofold rotational symmetry: it is found (Table 6) that bonds *a*, *c* and *e* are longer than bonds *b*, *f* and *d*, respectively, indicating beyond question that the canonical form (*F*) is the dominant contributor, rather than form (*G*). It is, moreover, significant that the exocyclic bond *g* is longer in (10) than in any of (3)–(8), where this bond always forms part of a delocalized five-centre, six-electron system.

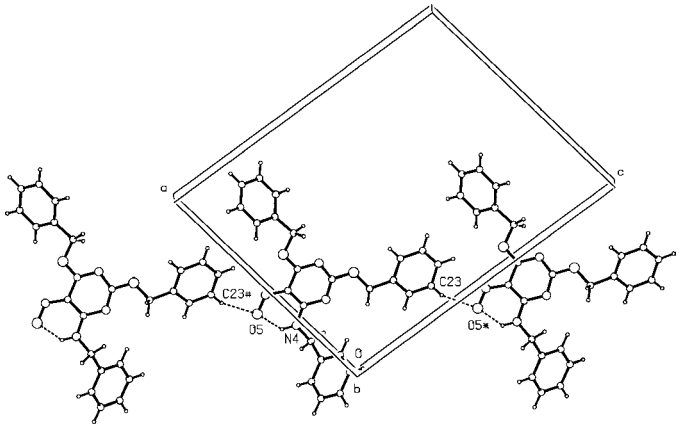

Figure 11
Part of the crystal structure of (8), showing the formation by the C—H···O hydrogen bonds of a $C(12)$ chain along [$\bar{1}$01]. The atoms marked with an asterisk (*) or hash (#) are at the symmetry positions $(-\frac{1}{2}+x, \frac{1}{2}-y, \frac{1}{2}+z)$ and $(\frac{1}{2}+x, \frac{1}{2}-y, -\frac{1}{2}+z)$, respectively.

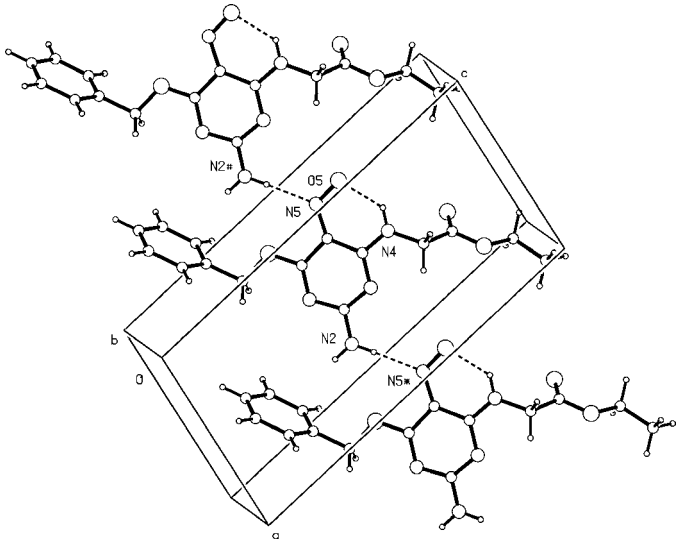

Figure 12
Part of the crystal structure of (4), showing the formation of a $C(7)$ chain along [100]. The atoms marked with an asterisk (*) or hash (#) are at the symmetry positions $(1+x, y, z)$ and $(-1+x, y, z)$, respectively.

Table 7
Hydrogen-bond geometry (Å, °).

D—H···*A*	H···*A*	*D*···*A*	*D*—H···*A*	Motif	Direction
(3)					
N14—H14···O15	1.97	2.630 (2)	131	$S(6)$	–
N24—H24···O25	1.96	2.636 (2)	133	$S(6)$	–
N12—H12*B*···N15^{i}	2.34	3.177 (2)	166	$C(7)$	[010]
N22—H22*B*···N25^{ii}	2.12	3.063 (2)	175	$C(7)$	[010]
(4)					
N4—H4···O5	1.96	2.623 (2)	131	$S(6)$	–
N2—H2*A*···N5^{iii}	2.12	2.987 (2)	171	$C(7)$	[100]
(5*A*)					
N4—H4···O5	1.93	2.603 (9)	133†	$S(6)$	–
N4—H4···O5^{iv}	2.40	3.223 (10)	156†	$R_2^2(4)$	‡
N2—H2*A*···N3^{v}	2.18	3.056 (9)	171	$R_2^2(8)$	‡
(5*B*)					
N14—H14···O15	1.95	2.628 (4)	133	$S(6)$	–
N24—H24···O25	1.93	2.616 (4)	134	$S(6)$	–
N12—H12*A*···N15^{iii}	2.17	3.042 (5)	174	$C(7)$	[100]
N22—H22*A*···N25^{vi}	2.14	3.023 (4)	176	$C(7)$	[100]
(6)					
N14—H14···O15	1.93	2.606 (3)	132	$S(6)$	–
N24—H24···O25	1.96	2.621 (4)	131	$S(6)$	–
N22—H22*B*···N15	2.48	3.302 (4)	155§	*D*	–
N22—H22*B*···O16	2.44	3.115 (3)	133§	*D*	–
N22—H22*A*···N25^{vi}	2.22	2.925 (4)	137¶	$C(7)$	[100]
N22—H22*A*···O25^{vi}	2.17	3.043 (4)	167¶	$C(8)$	[100]
N12—H12*A*···N15^{vii}	2.59	3.165 (4)	123††	$C(7)$	[010]
N12—H12*A*···O15^{vii}	2.15	2.962 (4)	153††	$C(8)$	[010]
N12—H12*B*···O26^{viii}	2.46	3.199 (4)	142	$C_2^2(12)$	[110]
(7)					
N14—H14···O15	1.94	2.605 (3)	131	$S(6)$	–
N24—H24···O25	1.97	2.626 (2)	131	$S(6)$	–
N22—H22···O15	2.07	2.853 (3)	148	*D*	–
N12—H12···O25^{ix}	2.09	2.875 (2)	149	$C_2^2(16)$	[101]
(8)					
N4—H4···O5	1.94	2.606 (2)	132	$S(6)$	–
C23—H23···O5^{x}	2.40	3.304 (2)	159	$C(12)$	[$\bar{1}$01]
(9)					
N2—H2···O5^{xi}	2.22	3.099 (2)	173‡‡	$C(8)$	[010]
N2—H2···N5^{xi}	2.28	3.023 (2)	143‡‡	$C(7)$	[010]
(10)					
N2—H2*A*···N1^{xii}	2.13	3.002 (2)	170	$R_2^2(8)$	–
N2—H2*B*···O4^{xiii}	2.27	3.013 (2)	141	$C(6)$	[001]
(11)					
N12—H12*B*···N21	2.30	3.163 (4)	166	*D*	§§
N22—H22*B*···N11	2.24	3.107 (4)	169	*D*	§§
N12—H12*A*···O15A^{xiv}	2.33	3.059 (4)	140	$R_2^2(16)$	–
N22—H22*A*···O1	2.02	2.870 (4)	163	*D*	–
O1—H11···O15*A*^{xv}	1.79	2.779 (4)	171¶¶	*D*	†††
O1—H11···N15*A*^{xv}	2.29	3.184 (5)	149¶¶	*D*	–
O1—H12···O25*A*^{xvi}	1.77	2.769 (4)	176‡‡‡	$R_4^4(20)$	–
O1—H12···N25*A*^{xvi}	2.24	3.109 (5)	145‡‡‡	$R_2^2(18)$	–

Symmetry codes: (i) $\frac{3}{2}-x, -\frac{1}{2}+y, \frac{1}{2}-z$; (ii) $\frac{5}{2}-x, \frac{1}{2}+y, \frac{1}{2}-z$; (iii) $1+x, y, z$; (iv) $-x, 1-y, -z$; (v) $2-x, 1-y, 1-z$; (vi) $-1+x, y, z$; (vii) $x, -1+y, z$; (viii) $-1+x, -1+y, z$; (ix) $1+x, y, 1+z$; (x) $-\frac{1}{2}+x, \frac{1}{2}-y, \frac{1}{2}+z$; (xi) $1-x, -\frac{1}{2}+y, \frac{3}{2}-z$; (xii) $1-x, y, -\frac{1}{2}-z$; (xiii) $x, 1-y, -\frac{1}{2}+z$; (xiv) $-x, 2-y, -z$; (xv) $\frac{1}{2}-x, -\frac{1}{2}+y, \frac{1}{2}-z$; (xvi) $1-x, 2-y, -z$. † Three-centre N—H···$(O)_2$ system: sum of angles at H4, 359°. ‡ Secondary network $C_2^2(12)$ $[R_2^2(4)][R_2^2(8)]$ parallel to [201]. § Three-centre N—H···(N,O) system: sum of angles at H22*B*, 353°. ¶ Three-centre N—H···(N,O) system: sum of angles at H22*A*, 338°. †† Three-centre N—H···(N,O) system: sum of angles at H12*A*, 306°. ‡‡ Three-centre N—H···(N,O) system: sum of angles at H2, 348°. §§ Secondary network $R_2^2(8)$. ¶¶ Three-centre N—H···(N,O) system: sum of angles at H2, 354°. ††† Secondary network $C_3^3(10)$ parallel to [010]. ‡‡‡ Three-centre N—H···(N,O) system: sum of angles at H2, 355°.

It is interesting to note that the general pattern of the bond lengths in the 5-nitrosopyrimidines (3)–(9) reported here, although highly unusual, is in fact entirely consistent with the pattern observed (Low *et al.*, 2000) in *N*-(6-amino-3,4-dihydro-

3-methyl-5-nitroso-4-oxopyrimidin-2-yl) derivatives (12) of a

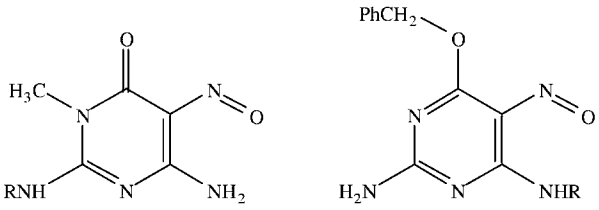

(12) (4) - (6)

range of amino acids, which, apart from carrying an alkyl group on N rather than on O, closely resemble the amino-acid derivatives (4)–(6).

That similar bond polarization occurs in both types of compound confirms the deductions made both here and earlier (Low *et al.*, 2000) that the enol-imidic [—N═C(OCH$_2$Ph)—] and amidic [—(CH$_3$)N—C(═O)—] fragments do not participate significantly in the bond-polarization process.

3.4. Supramolecular aggregation *via* hydrogen bonding

3.4.1. Hard hydrogen bonds form finite, zero-dimensional aggregates. In (8) (Fig. 7) the sole hard hydrogen bond present is the intramolecular N—H···O hydrogen bond forming the usual $S(6)$ motif. There are no other hard hydrogen-bond donors in the molecule: however, uniquely in this series, and possibly associated with the absence of hard intermolecular hydrogen bonds, there is a significant soft C—H···O hydrogen bond (Table 7). Aromatic C23 at (x, y, z) acts as a hydrogen-bond donor to nitroso O5 at $(-\frac{1}{2}+x, \frac{1}{2}-y, \frac{1}{2}+z)$, thus producing a $C(12)$ chain running parallel to the [101] direction and generated by the *n*-glide plane at $y = 0.25$ (Fig. 11). Thus, although the hard hydrogen bond is only intramolecular, the soft hydrogen bond generates a one-dimensional structure.

3.4.2. Hard hydrogen bonds generate one-dimensional structures.

Simple chains. Compounds (4) and (9) (Figs. 2 and 8) both crystallize with $Z' = 1$, in space groups $P\bar{1}$ and $P2_1/c$, respectively. Compound (4) contains the common $S(6)$ motif generated by the intramolecular N—H···O hydrogen bond and, in addition, N2 at (x, y, z) acts as a hydrogen-bond donor

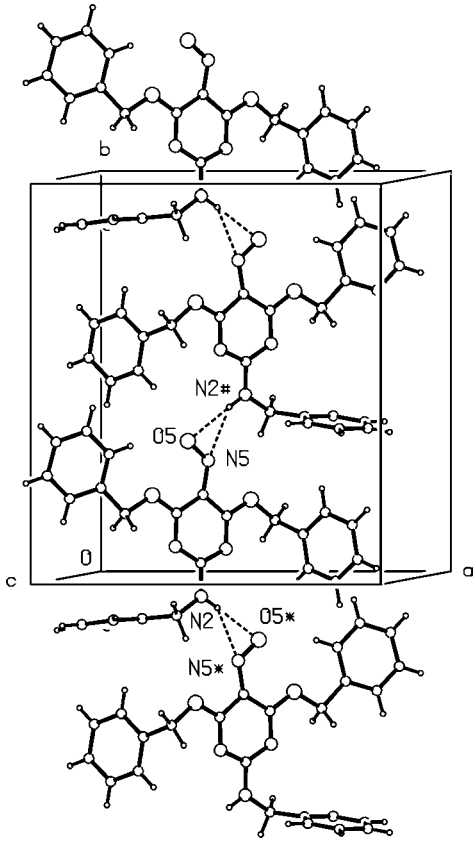

Figure 13
Part of the crystal structure of (9), showing the formation of a $C(7)/C(8)$ chain along [010]. The atoms marked with an asterisk (*) or hash (#) are at the symmetry positions $(1-x, -\frac{1}{2}+y, \frac{3}{2}-z)$ and $(1-x, \frac{1}{2}+y, \frac{3}{2}-z)$, respectively.

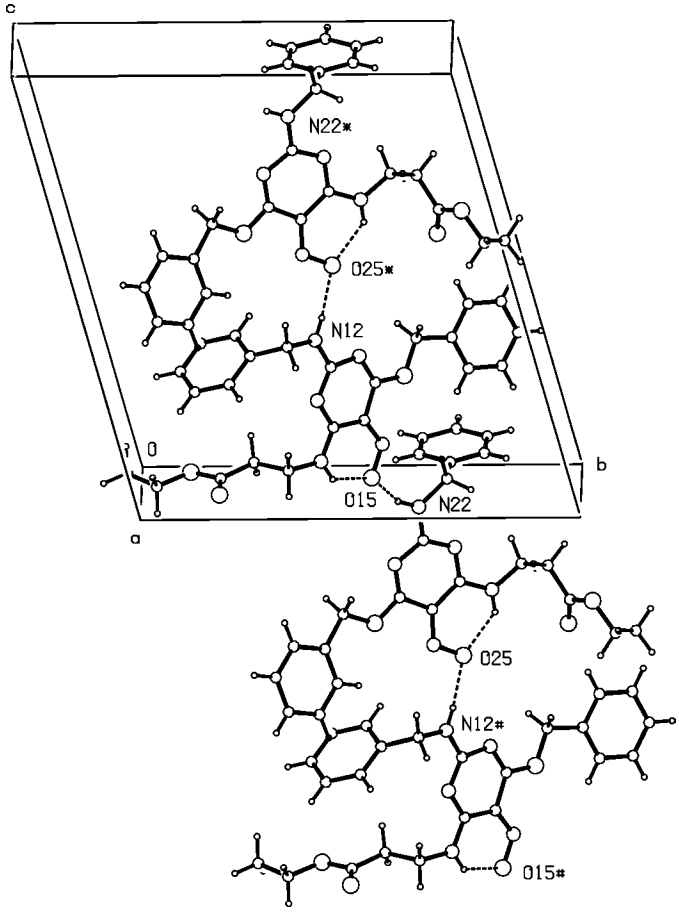

Figure 14
Part of the crystal structure of (7), showing the formation of a $C_2^2(16)$ chain along [101]. The atoms marked with an asterisk (*) or hash (#) are at the symmetry positions $(1+x, y, 1+z)$ and $(-1+x, y, -1+z)$, respectively.

to nitroso N5 at $(1+x, y, z)$, thus generating by translation a $C(7)$ chain running parallel to [100] (Fig. 12). The chain formation in (9) involves the nitroso O, rather than N, as an acceptor: N2 at (x, y, z) acts as a donor to O5 at $(1-x, -\frac{1}{2}+y, \frac{3}{2}-z)$, while N2 at $(1-x, -\frac{1}{2}+y, \frac{3}{2}-z)$ in turn acts as a donor to O5 at $(x, -1+y, z)$, thus producing a $C(8)$ chain parallel to [010] generated by the 2_1 screw axis along $(\frac{1}{2}, y, \frac{3}{4})$ (Fig. 13).

By contrast, (7) (Fig. 6) has $Z' = 2$ in space group $P\bar{1}$, but the chain formation is very similar to that in (9), in that the two independent molecules are linked by two N—H···O hydrogen bonds each having a nitroso O atom as an acceptor. Within the asymmetric unit (Fig. 6) N22 acts as a hydrogen-bond donor to O15: in similar fashion, N12 at (x, y, z) acts as a donor to O25 at $(1+x, y, 1+z)$, thus generating by translation a $C_2^2(16)$ chain running parallel to [101] (Fig. 14). In each of (4), (7) and (9) there are two chains running through each unit cell, related to one another by the centres of inversion and hence antiparallel.

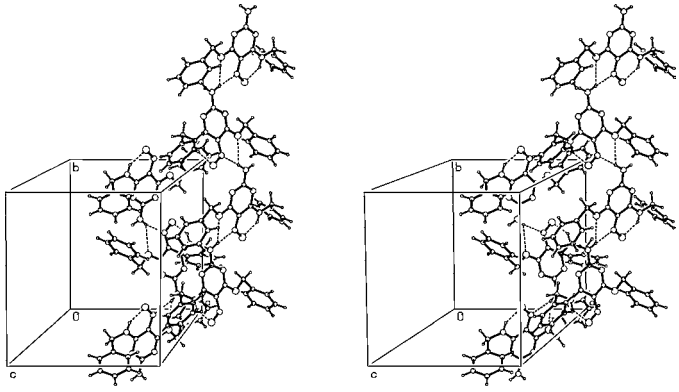

Figure 15
Stereoview of part of the crystal structure of (1), showing the formation of antiparallel $C(7)$ chains along [010].

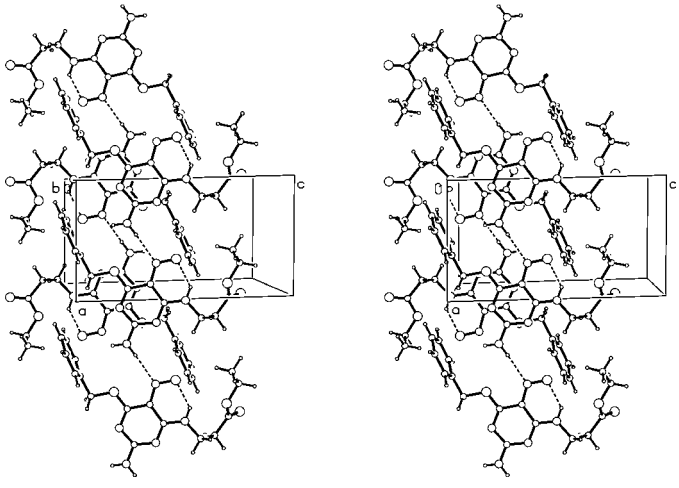

Figure 16
Stereoview of part of the crystal structure of (5*B*), showing the formation of antiparallel $C(7)$ chains along [100].

Paired chains. Compound (3) and polymorph (5*B*) of (5) crystallize with $Z' = 2$ in space groups $P2_1/n$ and $P2_1$, respectively, and in both structures each independent molecule forms a $C(7)$ chain. Thus, in (3) molecules of type 1 (Fig. 1) form a $C(7)$ chain parallel to [010] generated by the 2_1 axis along $(\frac{3}{4}, y, \frac{1}{2})$, while type 2 molecules form an antiparallel chain generated by the 2_1 axis along $(1.25, y, \frac{1}{4})$: N12 and N22 at (x, y, z) act as hydrogen bond donors, respectively, to nitroso N15 and N25 at $(\frac{3}{2}-x, -\frac{1}{2}+y, \frac{1}{2}-z)$ and $(\frac{5}{2}-x, \frac{1}{2}+y, \frac{1}{2}-z)$ (Fig. 15).

The chain formation in (5*B*) is very similar, except only that the chains are generated by translation along [100]: N12 and N22 at (x, y, z) (Fig. 4) act as hydrogen-bond donors, respectively, to N15 at $(1+x, y, z)$ and to N25 at $(-1+x, y, z)$ (Fig. 16). There are no hydrogen bonds between the two types of chain in either (3) or (5*B*).

A chain of rings. There are two intermolecular hydrogen bonds in polymorph (5*A*) of (5) (Fig. 3), in addition to the intramolecular N—H···O hydrogen bond having nitroso O as an acceptor. This intramolecular bond is, in fact, one component of a planar three-centre system, in which N4 is the hydrogen-bond donor and where the two acceptors are nitroso O5 within the same molecule at (x, y, z), and in the molecule at $(-x, 1-y, -z)$. The net result is the formation of the fused tricyclic hydrogen-bond system, in which the central ring is a rather unusual $R_2^2(4)$ motif centred at $(0, \frac{1}{2}, 0)$ (Fig. 17). In addition, N2 in the molecule at (x, y, z) acts as a hydrogen-bond donor, *via* H2*A*, to N3 at $(2-x, 1-y, 1-z)$, thus generating a second centrosymmetric ring, this time of $R_2^2(8)$ type, centred at $(1, \frac{1}{2}, \frac{1}{2})$ (Fig. 17). Propagation of these two centrosymmetric motifs generates a $C_2^2(12)$ $[R_2^2(4)]$ $[R_2^2(8)]$ chain of rings (Bernstein *et al.*, 1995) running parallel to the [201] direction (Fig. 17). It is interesting to note that H2*B*,

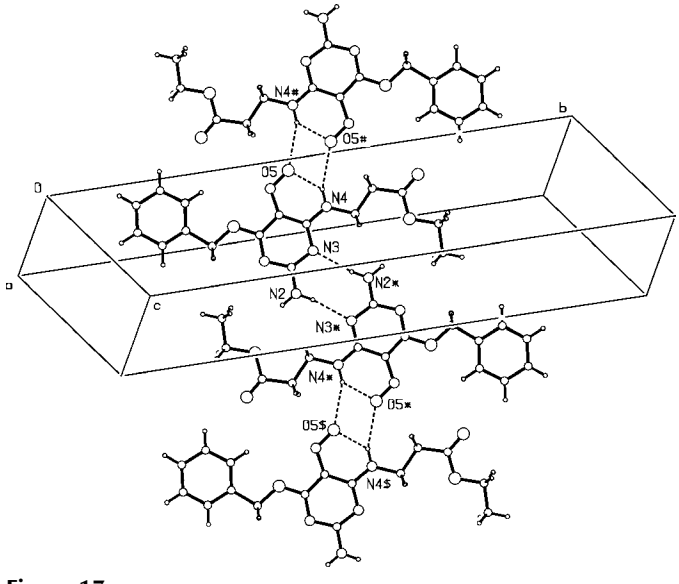

Figure 17
Part of the crystal structure of (5*A*), showing the formation of a chain of rings along [201]. The atoms marked with an asterisk (*), hash (#) or dollar sign ($) are at the symmetry positions $(2-x, 1-y, 1-z)$, $(-x, 1-y, -z)$ and $(2+x, y, 1+z)$, respectively.

bonded to N2, plays no part in the hydrogen bonding and that the $R_2^2(4)$ motif is apparently preferred to the formation of an N—H···O hydrogen bond involving H2*B*.

A molecular ladder. Compound (10) is unique amongst the compounds studied here in that the pyrimidine ring carries no nitroso group (Fig. 9). There are just two intermolecular hydrogen bonds, one each of N—H···N and N—H···O types, and the combined effect of these when propagated in space group *C*2/*c* is the generation of a molecular ladder. Amino N2 in the molecule at (x, y, z) acts as a hydrogen-bond donor, *via* H2*A*, to ring N1 in the molecule at ($1-x$, y, $-\frac{1}{2}-z$), while N2 at ($1-x$, y, $-\frac{1}{2}-z$) in turn acts as a donor to N1 at (x, y, z), thus producing an $R_2^2(8)$ ring generated by the twofold rotation axis along ($\frac{1}{2}$, y, $-\frac{1}{4}$) (Fig. 18). The same N2 at (x, y, z) also acts as a hydrogen-bond donor, this time *via* H2*B*, to O4 at (x, $1-y$, $-\frac{1}{2}+z$), while N2 at (x, $1-y$, $-\frac{1}{2}+z$) acts as a donor to O4 at (x, y, $-1+z$), thus producing a $C(6)$ chain running parallel to [001] and generated by the *c*-glide plane at $y = 0.5$ (Fig. 19).

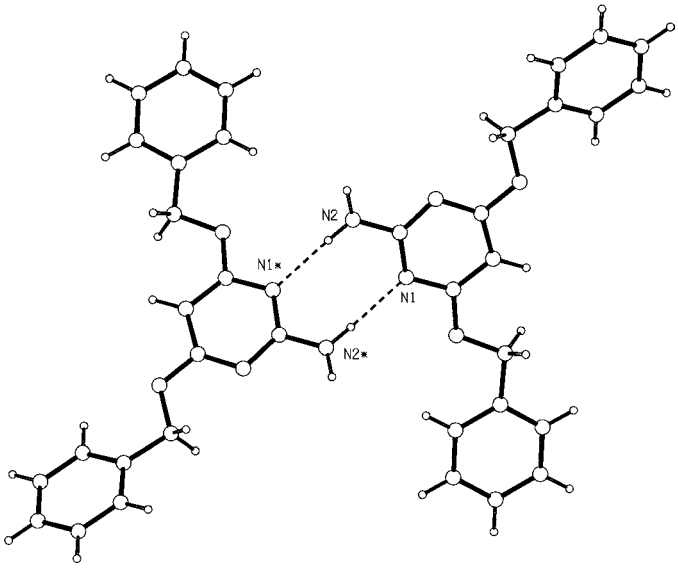

Figure 18
Part of the crystal structure of (10) showing the formation of a dimer lying across a twofold rotation axis. The atoms marked with an asterisk (*) are at the symmetry position ($1-x$, y, $-\frac{1}{2}-z$).

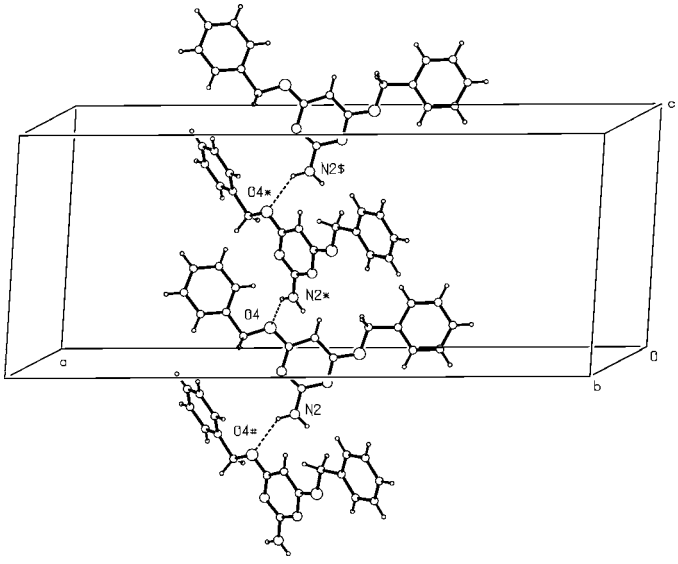

Figure 19
Part of the crystal structure of (10) showing the formation of a $C(6)$ chain parallel to [001]. The atoms marked with an asterisk (*), hash (#) or dollar sign ($) are at the symmetry positions (x, $1-y$, $\frac{1}{2}+z$), (x, $1-y$, $-\frac{1}{2}+z$) and (x, y, $1+z$), respectively.

The combination of these two motifs generates a molecular ladder, in which two antiparallel $C(6)$ chains, related to one another by the twofold rotation axes, form the uprights and pairs of molecules linked by the $R_2^2(8)$ rings act as the rungs; the scheme below emphasizes the interplay of hydrogen-bonding and benzyl conformation.

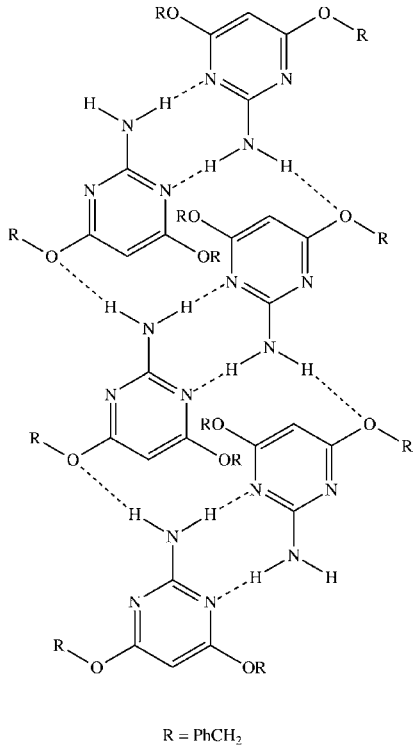

R = $PhCH_2$

Between these rungs there are $R_4^4(16)$ rings: the $R_2^2(8)$ rings lie across the rotation axes along ($\frac{1}{2}$, y, $n/2+\frac{1}{4}$) (n = zero or integer) and the $R_4^4(16)$ rings lie across inversion centres at ($\frac{1}{2}$, $\frac{1}{2}$, $n/2+\frac{1}{2}$) (n = zero or integer). There are two such ladders passing through each unit cell, one in the domain $0.26 < x < 0.74$ and the other in the domain $0.76 < x < 1.24$, but there are no hydrogen bonds between neighbouring ladders.

3.4.3. Hard hydrogen bonds generate a two-dimensional structure. The crystal structure of (6) (Fig. 5), which crystallizes in space group *P*1 with $Z' = 2$, is characterized by a large number of hydrogen bonds, both two-centred and three-centred, which link the two independent molecules into a two-dimensional network. Each of the molecules exhibits the usual $S(6)$ intramolecular N—H···O hydrogen bond with the nitroso O as an acceptor. It is striking that the two inter-

molecular hydrogen bonds formed by the amino group in the type 1 molecule are both two-centre N—H···O interactions, whereas each N—H bond of the amino group in the type 2 molecule participates in a three-centre system with one N and one O acceptor in each case.

The type 1 molecules are linked into a $C(8)$ chain parallel to [010] *via* a two-centre hydrogen bond, while the type 2 molecules are linked into a $C(8)$ chain parallel to [100] *via* a three-centre hydrogen bond. Amino N12 in the type 1 molecule at (x, y, z) acts as a hydrogen-bond donor, *via* H12*A*, to O15 and weakly to N15 in the type 1 molecule at $(x, -1 + y, z)$ (Fig. 20). In the type 2 molecules, amino N22 at (x, y, z) acts as a hydrogen-bond donor, *via* H22*A*, to both N25 and O25 at $(-1 + x, y, z)$: of the two individual components of this three-centre system, that involving O25 is much more nearly linear and counting *via* O25 leads to a $C(8)$ motif (Fig. 21).

The two sets of chains, parallel to [010] and [100], are linked into a continuous two-dimensional network by a three-centre hydrogen bond which links the two independent molecules within the asymmetric unit (Fig. 5), where amino N22 in the type 2 molecule acts as a donor, *via* H22*B*, to both N15 and O16 in the type 1 molecule. In this three-centre system, the interaction with the N acceptor is the more nearly linear, in contrast to that formed by H22*A*. The combination in this manner of the two types of chain generates a sheet parallel to (001) built from $R_8^8(44)$ rings, where in all three-centre systems the pathway is counted *via* the O acceptor.

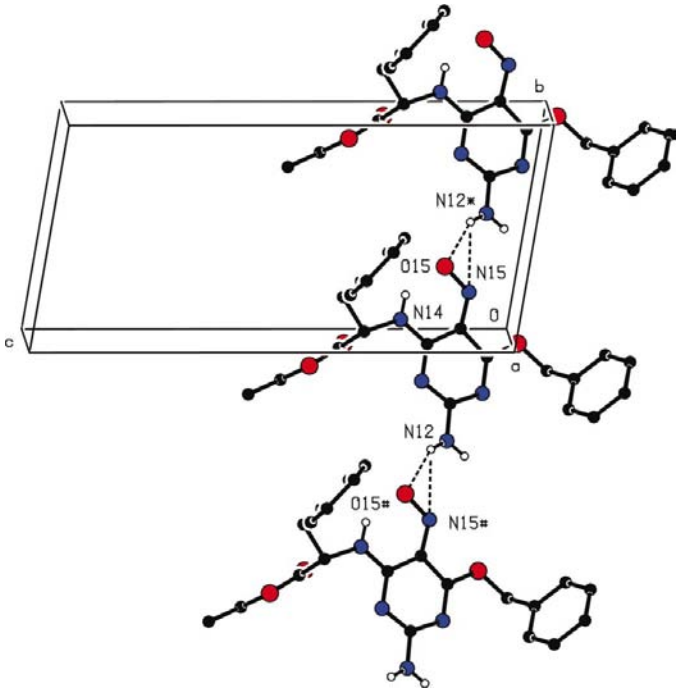

Figure 20
Part of the crystal structure of (6) showing the formation of a chain along [010] comprising type 1 molecules only. For the sake of clarity, H atoms bonded to C are omitted. The atoms marked with an asterisk (*) or hash (#) are at the symmetry positions $(x, 1 + y, z)$ and $(x, -1 + y, z)$, respectively.

Finally, in a further motif which involves both types of molecule, N12 in the type 1 molecule at (x, y, z) acts as a donor, *via* H12*B*, to O26 in the type 2 molecule at $(1 + x, 1 + y, z)$, thus generating a $C_2^2(12)$ chain parallel to [110] (Fig. 22). The effect of this motif is to subdivide the $R_8^8(44)$ rings of the (001) sheet into $R_4^4(16)$ and $R_6^6(34)$ sectors, and thereby to strengthen the sheet.

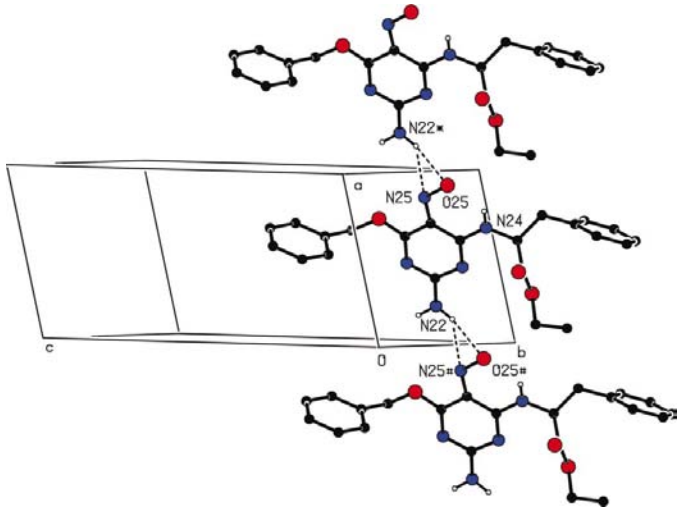

Figure 21
Part of the crystal structure of (6) showing the formation of a chain along [100] comprising type 2 molecules only. For the sake of clarity, H atoms bonded to C are omitted. The atoms marked with an asterisk (*) or hash (#) are at the symmetry positions $(1 + x, y, z)$ and $(-1 + x, y, z)$, respectively.

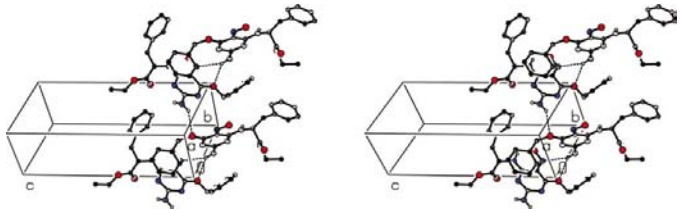

Figure 22
Stereoview of part of the crystal structure of (6) showing the formation of a $C_2^2(12)$ chain along [110] involving both types of molecule. For the sake of clarity, H atoms bonded to C are omitted.

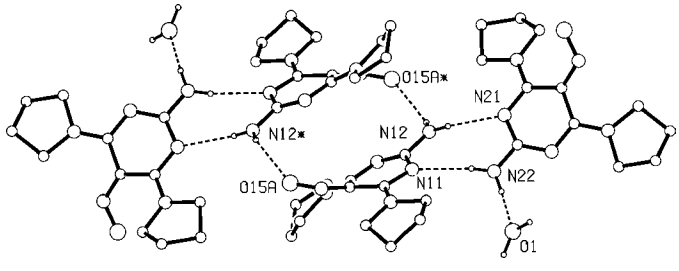

Figure 23
Part of the crystal structure of (11) showing the formation of a centrosymmetric six-molecule aggregate containing $R_2^2(8)$ and $R_2^2(16)$ rings. For the sake of clarity, only the major components are shown and H atoms bonded to C are omitted. The atoms marked with an asterisk (*) are at the symmetry position $(-x, 2 - y, -z)$.

3.4.4. Hard hydrogen bonds generate a three-dimensional structure. In (11) both of the nitroso groups are independently disordered each over two sets of sites (see §2.2), but only the major sites will be considered in the following analysis of the hydrogen bonding. Similarly, the minor-occupancy water molecule will not be considered further in this context. Subject to these constraints, the major components are linked into a three-dimensional framework.

Within the asymmetric unit of (11), N12 and N22 act as hydrogen-bond donors, *via* H12*B* and H22*B*, respectively, to N11 and N21, giving an $R_2^2(8)$ motif (Fig. 23) having approximate but not precise twofold rotational symmetry. In addition, N12 at (x, y, z) acts as a hydrogen-bond donor, *via* H12*A*, to O15A at $(-x, 2-y, -z)$, thus generating an $R_2^2(16)$ ring centred at (0, 1, 0), while N22 at (x, y, z) acts as a donor, *via* H22*A*, to O1 also at (x, y, z). In this manner a centrosymmetric six-molecule aggregate containing three rings is formed (Fig. 23).

The water molecule containing O1 acts as a hydrogen-bond donor in two independent three-centre systems (Table 7): O1 at (x, y, z) acts as a donor, *via* H11, to both O15*A* and N15*A* at $(\frac{1}{2}-x, -\frac{1}{2}+y, \frac{1}{2}-z)$, forming a $C_3^3(10)$ chain (counting *via* O15*A*, as this has the stronger interaction) running parallel to [010] (Fig. 24); O1 at (x, y, z) also acts as a donor *via* H12 to both O25*A* and N25A at $(1-x, 2-y, -z)$, thus generating an $R_4^4(20)$ ring (again counting *via* O, as this has the stronger interaction) centred at $(\frac{1}{2}, 1, 0)$ (Fig. 25). These two hydrogen bonds link each six-molecule aggregate (Fig. 23) to six others: thus, the aggregate centred at (0, 1, 0) is linked *via* the $C_3^3(10)$ chain motif to those centred at $(\frac{1}{2}, \frac{1}{2}, \frac{1}{2})$, $(\frac{1}{2}, \frac{3}{4}, \frac{1}{2})$, $(-\frac{1}{2}, \frac{1}{2}, -\frac{1}{2})$ and $(-\frac{1}{2}, \frac{3}{2}, -\frac{1}{2})$ so that propagation by the space group of this interaction generates a $(10\bar{1})$ sheet. Similarly, the aggregate centred at (0, 1, 0) is linked *via* the $R_4^4(20)$ ring motif to those centred at (1, 1, 0) and (−1, 1, 0), thus generating a chain of fused $R_2^2(8)$, $R_2^2(16)$ and $R_4^4(20)$ rings parallel to [100]. Propagation of these interactions and the combination of the [100] chain with the $(10\bar{1})$ sheet generates a continuous three-dimensional framework.

As noted above (§2.2), several analogues of (11) containing different dialkylamino substituents have been examined in an attempt to find an analogue whose structure is not bedevilled by multiple disorder, but none has been obtained in suitably crystalline form; this particular series seems particularly reluctant to form appropriately crystalline solids. Thus, to date, the structure of (11) is the sole representative of this class.

3.4.5. General comments on the hydrogen bonding. The hydrogen bonding observed in the nitroso (3)–(9) (Table 7, Figs. 11–17 and 20–22) is striking for the distribution of the hydrogen-bond donors and acceptors, as well as for the frequent occurrence of nearly planar three-centre $D-\mathrm{H}\cdots(A)_2$ systems in (5*A*), (6), (9) and (11). While the donors are exclusively the amino N substituents at positions 2- and/or 4- of the pyrimidine ring, the dominant acceptors are the N and/or O atoms of the nitroso groups. Only in polymorph (5*A*), where a ring N acts as an acceptor (Fig. 17), and in (6), where the O atoms at position 6 act as acceptors in both of the independent molecules, are any other acceptors involved. This general trend is entirely consistent with the polarized form adopted by all the nitroso derivatives (3)–(9) and hence most of the hard hydrogen bonds noted in Table 7 are charge assisted (Gilli *et al.*, 1994). Since few of the intermolecular hydrogen bonds have short $D\cdots A$ distances, it may well be that in the absence of the charge assistance induced by the polarized electronic structures, the intermolecular hydrogen bonding would be considerably less extensive.

4. Conclusions

The structures reported here for nitrosopyrimidines (3)–(9) all exhibit strong polarization of the electronic structures, as

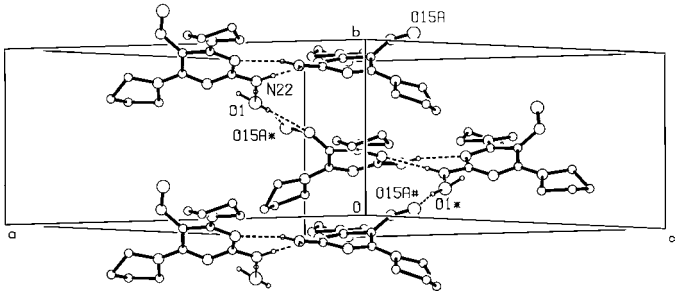

Figure 24
Part of the crystal structure of (11) showing the formation of a $C_3^3(10)$ chain along [010]. For the sake of clarity, only the major components are shown and H atoms bonded to C are omitted. The atoms marked with an asterisk (*) or hash (#) are at the symmetry positions $(\frac{1}{2}-x, -\frac{1}{2}+y, \frac{1}{2}-z)$ and $(x, -1+y, z)$, respectively.

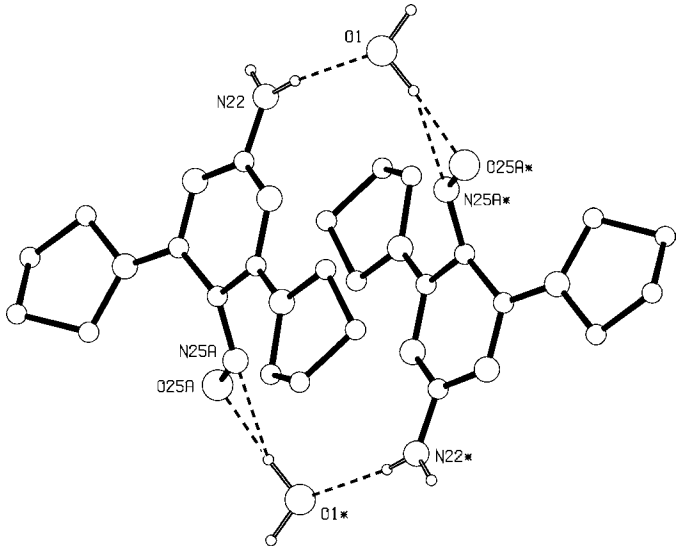

Figure 25
Part of the crystal structure of (11) showing the formation of a centrosymmetric four-molecule aggregate containing an $R_4^4(20)$ ring. For the sake of clarity, only the major components are shown and H atoms bonded to C are omitted. The atoms marked with an asterisk (*) are at the symmetry position $(1-x, 2-y, -z)$.

found earlier (Low *et al.*, 2000) for a series of related dihydropyrimidinones. Although the intramolecular distances are unusual in comparison with those in simple nitroso-arenes and in analogous pyrimidines carrying no nitroso substituent, a simple polarization model is consistent with all the present observations. At the same time, in (11), although the structure is heavily disordered, it is clear that the presence of two secondary amino substituents adjacent to the nitroso group is sufficient to cause severe non-planarity, with a consequent reduction in electronic delocalization.

X-ray data were collected at the EPSRC X-ray Crystallographic Service, University of Southampton, England, using a Nonius Kappa-CCD diffractometer: the authors thank the staff for all their help and advice. AQ thanks the Ministry of Education (Spain) for funding in support of his Semester of study in the University of Dundee, and JNL thanks NCR Self-Service, Dundee, for grants which have provided computing facilities for this work.

References

Abril, N., Luque-Romero, F. L., Christians, F. C., Encell, L. P., Loeb, L. A. & Pueyo, C. (1999). *Carcinogenesis*, **20**, 2089–2094.
Bauer, S. H. & Andreassen, A. L. (1972). *J. Phys. Chem.* **76**, 3099–3108.
Bernstein, J., Davis, R. E., Shimoni, L. & Chang, N.-L. (1995). *Angew. Chem. Int. Ed. Engl.* **34**, 1555–1573.
Blessing, R. H. (1995). *Acta Cryst.* A**51**, 33–37.
Blessing, R. H. (1997). *J. Appl. Cryst.* **30**, 421–426.
Chae, M. Y., McDougall, M. G., Dolan, M. E., Swenn, K., Pegg, A. E. & Moschel, R. C. (1995). *J. Med. Chem.* **38**, 359–365.
Davis, M. I., Boggs, J. E., Coffey, D. & Hanson, H. P. (1965). *J. Phys. Chem.* **69**, 3727–3730.
Ferguson, G. (1999). *PRPKAPPA*. University of Guelph, Canada.
Flack, H. D. (1983). *Acta Cryst.* A**39**, 876–881.
Flack, H. D. & Bernardinelli, G. (2000). *J. Appl. Cryst.* **33**, 1143–1148.
Friedman, H. S., Kokkinakis, D. M., Pluda, J., Friedman, A. H., Cokgor, I., Haglund, M. M., Ashley, D. M., Rich, J. N., Dolan, M. E., Pegg, A. E., Moschel, R. C., McLendon, R. E., Kerby, T., Herdon, J. E., Bigner, D. D. & Scold, S. C. (1998). *J. Clin. Oncol.* **16**, 3570–3575.
Gilli, P., Bertolasi, V., Ferretti, V. & Gilli, G. (1994). *J. Am. Chem. Soc.* **116**, 909–915.
Lister, J. H. (1996). *The Purines, Suppl. 1; The Chemistry of Heterocyclic Compounds*, edited by E. C. Taylor, Vol. 54, pp. 44–50. New York: John Wiley and Sons.
Low, J. N., López, M. D., Arranz Mascarós, P., Cobo Domingo, J., Godino, M. L., López Garzón, R., Gutiérrez, M. D., Melguizo, M., Ferguson, G. & Glidewell, C. (2000). *Acta Cryst.* B**56**, 882–892.
Marchal, A., Sánchez, A., Nogueras, M. & Melguizo, M. (1998). 18th European Colloquium on Heterocyclic Chemistry, Rouen, France. Abstract B-42.
Marchal, A., Sánchez, A., Nogueras, M. & Melguizo, M. (2000). 7th Ibn Sina International Conference on Pure and Applied Heterocyclic Chemistry, Alexandría, Egypt. Abstract P-214.
Nonius (1997). *Kappa-CCD Server Software*. Windows 3.11 Version, Nonius B.V., Delft, The Netherlands.
Otwinowski, Z. & Minor, W. (1997). *Methods Enzymol.* **276**, 307–326.
Quesada, A., Marchal, A., Sánchez, A., Nogueras, M. & Melguizo, M. (2000). XIXth European Colloquium on Heterocyclic Chemistry, Aveiro, Portugal. Abstracts, p. 227.
Schlemper, E. O., Murmann, R. K. & Hussain, M. S. (1986). *Acta Cryst.* C**42**, 1739–1743.
Sheldrick, G. M. (1997*a*). *SHELXL*97. University of Göttingen, Germany.
Sheldrick, G. M. (1997*b*). *SHELXS*97. University of Göttingen, Germany.
Spek, A. L. (2001). *PLATON*. Version of May 2001. University of Utrecht, The Netherlands.
Talberg, H. J. (1977). *Acta Chem. Scand. A*, **31**, 485–491.
Wilson, A. J. C. (1976). *Acta Cryst.* A**32**, 994–996.